ELECTRONIC SUPPLEMENTARY INFORMATION

Cation-Directed Synthetic Strategy Using 4f Tungstoantimonates as Nonlacunary Precursors for the Generation of 3d–4f Clusters

Elias Tanuhadi[†], Emir Al-Sayed[†], Ghenadie Novitchi[⊥], Alexander Roller[‡], Gerald Giester[§], and Annette Rompel[*, †]

[*]correspondence to annette.rompel@univie.ac.at

† Universität Wien, Fakultät für Chemie, Institut für Biophysikalische Chemie, 1090 Wien, Austria www.bpc.univie.ac.at.

‡ Universität Wien, Fakultät für Chemie, Zentrum für Röntgenstrukturanalyse, 1090 Wien, Austria

§ Universität Wien, Fakultät für Geowissenschaften, Geographie und Astronomie, Institut für Mineralogie und Kristallographie, 1090 Wien, Austria

⊥ Laboratoire National des Champs Magnetiques Intenses, CNRS, 25 rue des Martyrs, 38042 Grenoble Cedex 9, France.

Content

General Information

All reagents and chemicals were of high-purity grade and were used as purchased without further purification. $Na_9[B\text{-}\alpha\text{-}SbW_9O_{33}]$ and $Na_{16}(NH_4)[\{Y(\alpha\text{-}SbW_9O_{31}(OH)_2)(CH_3COO)(H_2O)\}_3(WO_4)] \cdot 48H_2O$ were prepared according to literature procedures.[1, 2]

Attenuated total reflection Fourier−transform Infrared Spectroscopy: All spectra were recorded on a Bruker Tensor 27 IR Spectrometer equipped with a single−reflection diamond−ATR unit. Frequencies are given in cm^{-1}, intensities denoted as w = weak, m = medium, s = strong.

UV–Vis spectroscopy: UV−Vis spectra were collected on a Shimadzu UV 1800 spectrophotometer.

Elemental analysis: Elemental analysis was performed with an iCAP 6500 series inductively coupled plasma-optical emission spectrometry (ICP-OES) spectrometer (Thermo Scientific, USA). The ICP-OES was equipped with a standard sample introduction system consisting of a concentric nebulizer and a cyclonic spray chamber. Transportation of sample solutions was performed by the peristaltic pump of the iCAP 6500 coupled to an ASX-520 auto sampler (Cetac, USA). Per element two sensitive and non-interfered emission lines were used, the first line for measurement and the second line for quality control.

Powder X-ray diffraction (*PXRD*) was performed on a Bruker D8 ADVANCE diffractometer, Cu Kα radiation, λ = 1.54056 Å, LYNXEYE silicon strip detector and SolX energy dispersive detector, variable slit aperture with 12 mm, $8° \leq 2\theta \leq 50°$.

Single crystal X-ray diffraction (SXRD): The X-ray data of **$NaLnSbW_9$** were measured on a Bruker X8 Apex2 diffractometer equipped with multilayer monochromators, Mo K/α(λ=0.71073Å) INCOATEC micro focus sealed tubes and Oxford cooling system. Data collection of **$KLnTMSbW_9$** was performed on a Bruker D8 VENTURE equipped with a multilayer monochromator, Mo Kα Incoatec Microfocus sealed tube, and Kryoflex cooling device (Ln = Tb^{III}, Dy^{III}, Ho^{III}, Er^{III}; TM = Co^{II}, Ni^{II}). The structures were solved by direct methods and refined by full-matrix least-squares. Non hydrogen atoms were refined with anisotropic displacement parameters. The following software was used for the structure-solving procedure: frame integration, Bruker SAINT software package using a narrow-frame algorithm (absorption correction)[3], SADABS[4], SHELXS-2013[5] (structure solution), SHELXL-2013[6] (refinement), OLEX2[7] (structure solution, refinement, molecular diagrams and graphical user-interface), and SHELXLE[8] (molecular diagrams and graphical user interface). CCDC-codes are provided in **Table S4**. Experimental data can be found in **Tables S5-S28.**

Magnetic Studies: Dc magnetic susceptibility data (2-300K) were collected on powdered samples using a SQUID magnetometer (Quantum Design MPMS-XL), applying a magnetic field of 0.1 T. All data were corrected for the contribution of the sample holder and the diamagnetism of the samples estimated from Pascal's constants.[9, 10] The field dependence of the magnetization (up to 5 T) was measured between 2.0 and 5.0 K. ac magnetic susceptibility was measured between 2 and 7 K with an oscillating field magnitude of Hac = 3.0 Oe and frequency ranging between 1 and 1488Hz in presence of a dc field up to Hdc = 4000 Oe. The relaxation times were extracted from simultaneous fit of χ'ac and χ"ac using generalized Debye model.[11] Fitting of the variable parameters and estimation of errors was

performed with lsq curve fit solver in MATLAB, jacobian matrix was used to generate 95% confidence intervals on the fitted parameters.

Experimental Procedure

Synthesis of non-lacunary 4f-precursors

Synthesis of $Na_{21}[(Tb(H_2O)(OH)_2(CH_3COO))_3(WO_4)(SbW_9O_{33})_3] \cdot 62\ H_2O$ (**$NaTbSbW_9$**):
$Na_9[SbW_9O_{33}]$•19.5 H_2O (0.602 g, 0.213 mmol) was dissolved in a mixture of 10 mL NaOAC [2M] pH 5.5 and 5 mL H_2O. $Tb(NO_3)_3$•5H_2O (0.087 g, 0.201 mmol) was added to the stirred solution and the resulting reaction mixture was heated to 80°C and stirred for 2 h giving a colorless solution. Slow evaporation of the resulting reaction mixture at 18°C gave colorless block shaped crystals over a period of 2 weeks. Yield: 1.4 g, 74 % based on Tb. Elem. Anal. calcd (found) for $Na_{21}Tb_3Sb_3W_{28}O_{174}H_{137}$ ($Na_{21}[(Tb(H_2O)(OH)_2(CH_3COO))_3(WO_4)(SbW_9O_{33})_3] \cdot 62\ H_2O$): Na 5.14 (7.34), Sb 3.89 (3.28), W 54.79 (45.10), Tb 5.08 (4.19).

Synthesis of $Na_{21}[(Dy(H_2O)(OH)_2(CH_3COO))_3(WO_4)(SbW_9O_{33})_3] \cdot 116\ H_2O$ (**$NaDySbW_9$**):
The synthesis of **$NaDySbW_9$** was similar to that of **$NaTbSbW_9$** except that $Tb(NO_3)_3$•5 H_2O was replaced by $Dy(NO_3)_3$•5 H_2O (0.07 g, 0.201 mmol). Colorless block shaped crystals were obtained after approximately 2 weeks. Yield: 1.08 g, 52 % based on Dy. Elem. Anal. calcd (found) for $Na_{21}Dy_3Sb_3W_{28}O_{228}H_{245}$ ($Na_{21}[(Dy(H_2O)(OH)_2(CH_3COO))_3(WO_4)(SbW_9O_{33})_3] \cdot 116\ H_2O$): Na 4.65 (6.08), Sb 3.52 (3.68), W 49.60 (49.90), Dy 4.70 (4.66).

Synthesis of $Na_{21}[(Ho(H_2O)(OH)_2(CH_3COO))_3(WO_4)(SbW_9O_{33})_3] \cdot 72\ H_2O$ (**$NaHoSbW_9$**):
The synthesis of **$NaHoSbW_9$** was similar to that of **$NaTbSbW_9$** except that $Tb(NO_3)_3$•5 H_2O was replaced by $Ho(NO_3)_3$•5 H_2O (0.089 g, 0.201 mmol). Pink block shaped crystals were obtained after approximately 2 weeks. Yield: 1.23 g, 64 % based on Ho. Elem. Anal. calcd (found) for $Na_{21}Ho_3Sb_3W_{28}O_{184}H_{157}$ ($Na_{21}[(Ho(H_2O)(OH)_2(CH_3COO))_3(WO_4)(SbW_9O_{33})_3] \cdot 72\ H_2O$): Na 5.03 (5.78), Sb 3.81 (3.26), W 53.66 (47.80), Ho 5.16 (4.34).

Synthesis of $Na_{21}[(Er(H_2O)(OH)_2(CH_3COO))_3(WO_4)(SbW_9O_{33})_3] \cdot 87\ H_2O$ (**$NaErSbW_9$**):
The synthesis of **$NaErSbW_9$** was similar to that of **$NaTbSbW_9$** except that $Tb(NO_3)_3$•5 H_2O was replaced by $Er(NO_3)_3$•5H_2O (0.089 g, 0.201 mmol). Pink block shaped crystals were obtained after approximately 2 weeks. Yield: 1.39 g, 70 % based on Er. Elem. Anal. calcd (found) for $Na_{21}Er_3Sb_3W_{28}O_{199}H_{185}$ ($Na_{21}[(Er(H_2O)(OH)_2(CH_3COO))_3(WO_4)(SbW_9O_{33})_3] \cdot 87\ H_2O$): Na 4.89 (5.23), Sb 3.70 (3.25), W 52.17 (44.00), Er 5.09 (4.35).

Synthesis of 3d-4f compounds using non-lacunary 4f-precursors

Synthesis of $K_5Na_{12}H_3[Ni(H_2O)Tb_3(H_2O)_5(W_3O_{11})(SbW_9O_{33})_3]$ • 94 H_2O (**$KNiTbSbW_9$**):

$NaTbSbW_9$ (0.118 g, 0.0126 mmol) was dissolved in 5 ml of a 2:1 mixture of KOAc/NaOAc (5 % v/v) and H_2O. To the resulting solution, $NiCl_2$•6 H_2O (0.009 g, 0.0372 mmol) and 20 µL of a K_2CO_3 [2 M] solution were added and the reaction mixture was heated to 50°C for 1.5 h. Slow evaporation at 18°C gave light green block shaped crystals after 2 days. Yield: 0.114 g, 86 % based on W. Elem. Anal. calcd (found) for $K_5Na_{12}NiTb_3Sb_3W_{30}O_{215}H_{213}$ ($K_5Na_{12}H_3[Ni(H_2O)Tb_3(H_2O)_5(W_3O_{11})(SbW_9O_{33})_3]$ • 99 H_2O): K 1.85 (2.04), Na 2.62 (5.54), Sb 3.47 (3.27), W 52.32 (47.70), Tb 4.52 (3.40), Ni 0.56 (0.71).

Synthesis of $K_5Na_{12}H_3[Ni(H_2O)Dy_3(H_2O)_5(W_3O_{11})(SbW_9O_{33})_3]$ • 110 H_2O (**$KNiDySbW_9$**)

The synthesis of **$KNiDySbW_9$** was similar to that of **$KNiTbSbW_9$** except that **$NaTbSbW_9$** was replaced by **$NaDySbW_9$** (0.131 g, 0.0126 mmol). Light green block shaped crystals were obtained after approximately 2 days. Yield: 0.109 g, 80 % based on W. Elem. Anal. calcd (found) for $K_5Na_{12}NiDy_3Sb_3W_{30}O_{231}H_{245}$ ($K_5Na_{12}H_3[Ni(H_2O)Dy_3(H_2O)_5(W_3O_{11})(SbW_9O_{33})_3]$ • 115 H_2O): K 1.80 (2.22), Na 2.54 (3.16), Sb 3.37 (3.03), W 50.87 (42.30), Dy 4.50 (3.51), Ni 0.54 (0.62).

Synthesis of $K_5Na_{12}H_3[Ni(H_2O)Ho_3(H_2O)_5(W_3O_{11})(SbW_9O_{33})_3]$ • 81 H_2O (**$KNiHoSbW_9$**)

The synthesis of **$KNiHoSbW_9$** was similar to that of **$KNiTbSbW_9$** except that **$NaTbSbW_9$** was replaced by **$NaHoSbW_9$** (0.121 g, 0.0126 mmol). Light green block shaped crystals were obtained after approximately 2 days. Yield: 0.110 g, 84 % based on W. Elem. Anal. calcd (found) for $K_5Na_{12}NiHo_3Sb_3W_{30}O_{202}H_{187}$ ($K_5Na_{12}H_3[Ni(H_2O)Ho_3(H_2O)_5(W_3O_{11})(SbW_9O_{33})_3]$ • 86 H_2O): K 1.89 (2.04), Na 2.67 (4.98), Sb 3.54 (3.41), W 53.41 (48.90), Ho 4.79 (3.84), Ni 0.57 (0.73).

Synthesis of $K_5Na_{12}H_3[Ni(H_2O)Er_3(H_2O)_5(W_3O_{11})(SbW_9O_{33})_3]$ • 63 H_2O (**$KNiErSbW_9$**)

The synthesis of **$KNiErSbW_9$** was similar to that of **$KNiTbSbW_9$** except that **$NaTbSbW_9$** was replaced by **$NaErSbW_9$** (0.124 g, 0.0126 mmol). Light green block shaped crystals were obtained after approximately 2 days. Yield: 0.087 g, 69 % based on W. Elem. Anal. calcd (found) for $K_5Na_{12}NiEr_3Sb_3W_{30}O_{184}H_{151}$ ($K_5Na_{12}H_3[Ni(H_2O)Er_3(H_2O)_5(W_3O_{11})(SbW_9O_{33})_3]$ • 68 H_2O): K 1.95 (1.86), Na 2.76 (4.35), Sb 3.65 (3.79), W 55.11 (52.60), Er 5.01 (2.72), Ni 0.59 (1.17).

Synthesis of $K_5Na_{12}H_3[Co(H_2O)Tb_3(H_2O)_5(W_3O_{11})(SbW_9O_{33})_3]$ • 63 H_2O (**$KCoTbSbW_9$**)

$NaTbSbW_9$ (0.118 g, 0.0126 mmol) was dissolved in 5 ml of a 2:1 mixture of KOAc/NaOAc (5% v/v) and H_2O. To the resulting solution, $CoCl_2$•6 H_2O (0.009 g, 0.0372 mmol) and 20 µL of a K_2CO_3 [2 M] solution were added and the pink reaction mixture was heated to 50°C for 1.5 h. Slow evaporation at 18°C gave light pink block shaped crystals after 2 days. Yield: 0.091 g, 72 % based on W. Elem. Anal. calcd (found) for $K_5Na_{12}CoTb_3Sb_3W_{30}O_{184}H_{151}$

($K_5Na_{12}H_3[Co(H_2O)Tb_3(H_2O)_5(W_3O_{11})(SbW_9O_{33})_3]$ • 68 H_2O): K 1.96 (2.46), Na 2.76 (5.22), Sb 3.65 (3.39), W 55.24 (49.40), Tb 4.78 (4.18), Co 0.59 (0.59).

Synthesis of $K_5Na_{12}H_3[Co(H_2O)Dy_3(H_2O)_5(W_3O_{11})(SbW_9O_{33})_3]$ • 57 H_2O (**$KCoDySbW_9$**)

The synthesis of **$KCoDySbW_9$** was similar to that of **$KCoTbSbW_9$** except that **$NaTbSbW_9$** was replaced by **$NaDySbW_9$** (0.131 g, 0.0126 mmol). Light pink block shaped crystals were obtained after approximately 2 days. Yield: 0.107 g, 86 % based on W. Elem. Anal. calcd (found) for $K_5Na_{12}CoDy_3Sb_3W_{30}O_{178}H_{139}$ ($K_5Na_{12}H_3[Co(H_2O)Dy_3(H_2O)_5(W_3O_{11})(SbW_9O_{33})_3]$ • 62 H_2O): K 1.98 (2.43), Na 2.79 (4.31), Sb 3.69 (3.70), W 55.79 (51.30), Dy 4.93 (4.62), Co 0.60 (0.63).

Synthesis of $K_5Na_{12}H_3[Co(H_2O)Ho_3(H_2O)_5(W_3O_{11})(SbW_9O_{33})_3]$ • 55 H_2O (**$KCoHoSbW_9$**)

The synthesis of **$KCoHoSbW_9$** was similar to that of **$KCoTbSbW_9$** except that **$NaTbSbW_9$** was replaced by **$NaHoSbW_9$** (0.121 g, 0.0126 mmol). Light pink block shaped crystals were obtained after approximately 2 days. Yield: 0.092 g, 74 % based on W. Elem. Anal. calcd (found) for $K_5Na_{12}CoHo_3Sb_3W_{30}O_{176}H_{135}$ ($K_5Na_{12}H_3[Co(H_2O)Ho_3(H_2O)_5(W_3O_{11})(SbW_9O_{33})_3]$ • 60 H_2O): K 1.98 (2.39), Na 2.80 (4.01), Sb 3.71 (3.66), W 55.95 (53.20), Ho 5.02 (4.65), Co 0.60 (0.63).

Synthesis of $K_5Na_{12}H_3[Co(H_2O)Er_3(H_2O)_5(W_3O_{11})(SbW_9O_{33})_3]$ • 64 H_2O (**$KCoErSbW_9$**)

The synthesis of **$KCoErSbW_9$** was similar to that of **$KCoTbSbW_9$** except that **$NaTbSbW_9$** was replaced by **$NaErSbW_9$** (0.124 g, 0.0126 mmol). Light pink block shaped crystals were obtained after approximately 2 days. Yield: 0.088 g, 70 % based on W. Elem. Anal. calcd (found) for $K_5Na_{12}CoEr_3Sb_3W_{30}O_{185}H_{153}$ ($K_5Na_{12}H_3[Co(H_2O)Er_3(H_2O)_5(W_3O_{11})(SbW_9O_{33})_3]$ • 69 H_2O): K 1.95 (2.45), Na 2.75 (4.19), Sb 3.64 (3.70), W 55.01 (49.30), Er 5.00 (4.81), Co 0.59 (0.63).

Synthesis of $K_5Na_{12}H_3[Co(H_2O)Y_3(H_2O)_5(W_3O_{11})(SbW_9O_{33})_3]$ • 46 H_2O (**$KCoYSbW_9$**)

$Na_{16}(NH_4)[\{Y(\alpha\text{-}SbW_9O_{31}(OH)_2)(CH_3COO)(H_2O)\}_3(WO_4)]_3$ 48 H_2O (0.337 g, 0.0378 mmol) was dissolved in 15 ml of a 2:1 mixture of KOAc/NaOAc (5% v/v) and H_2O. To the resulting solution, $CoCl_2$•$6H_2O$ (0.027 g, 0.1116 mmol) and 120 µL of a K_2CO_3 [2 M] solution were added and the reaction mixture was heated to 50°C for 1.5 h. Slow evaporation at 18°C gave light green block shaped crystals after 2 days. Yield: 0.290 g, 81 % based on W. Elem. Anal. calcd (found) for $K_5Na_{12}CoY_3Sb_3W_{30}O_{167}H_{117}$ ($K_5Na_{12}H_3[Co(H_2O)Y_3(H_2O)_5(W_3O_{11})(SbW_9O_{33})_3]$ • 51H_2O): K 2.06 (2.26), Na 2.91 (2.75), Sb 3.86 (3.86), W 58.26 (56.40), Y 2.82 (2.61), Co 0.62 (0.70).

IR-spectra

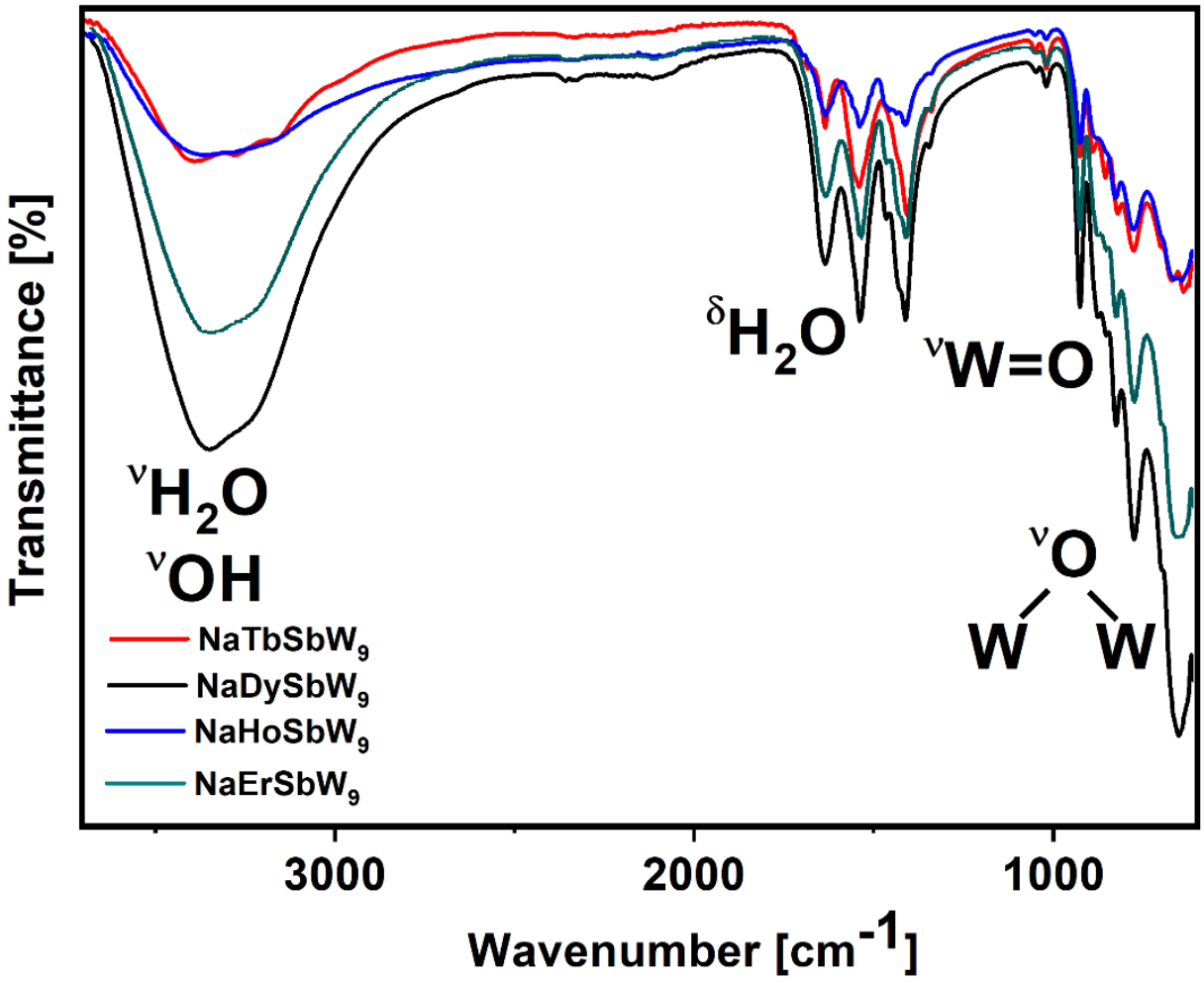

Figure S1. IR-spectra of **NaLnSbW$_9$** (ATR-IR, cm^{-1}): 3364.4 (s), 3263.6 (s), 2359.4 (w), 1637.8 (w), 1508.1 (m), 1401.6(m), 1234.6 (m), 1151.6 (w), 936.4 (w), 748.5 (m)

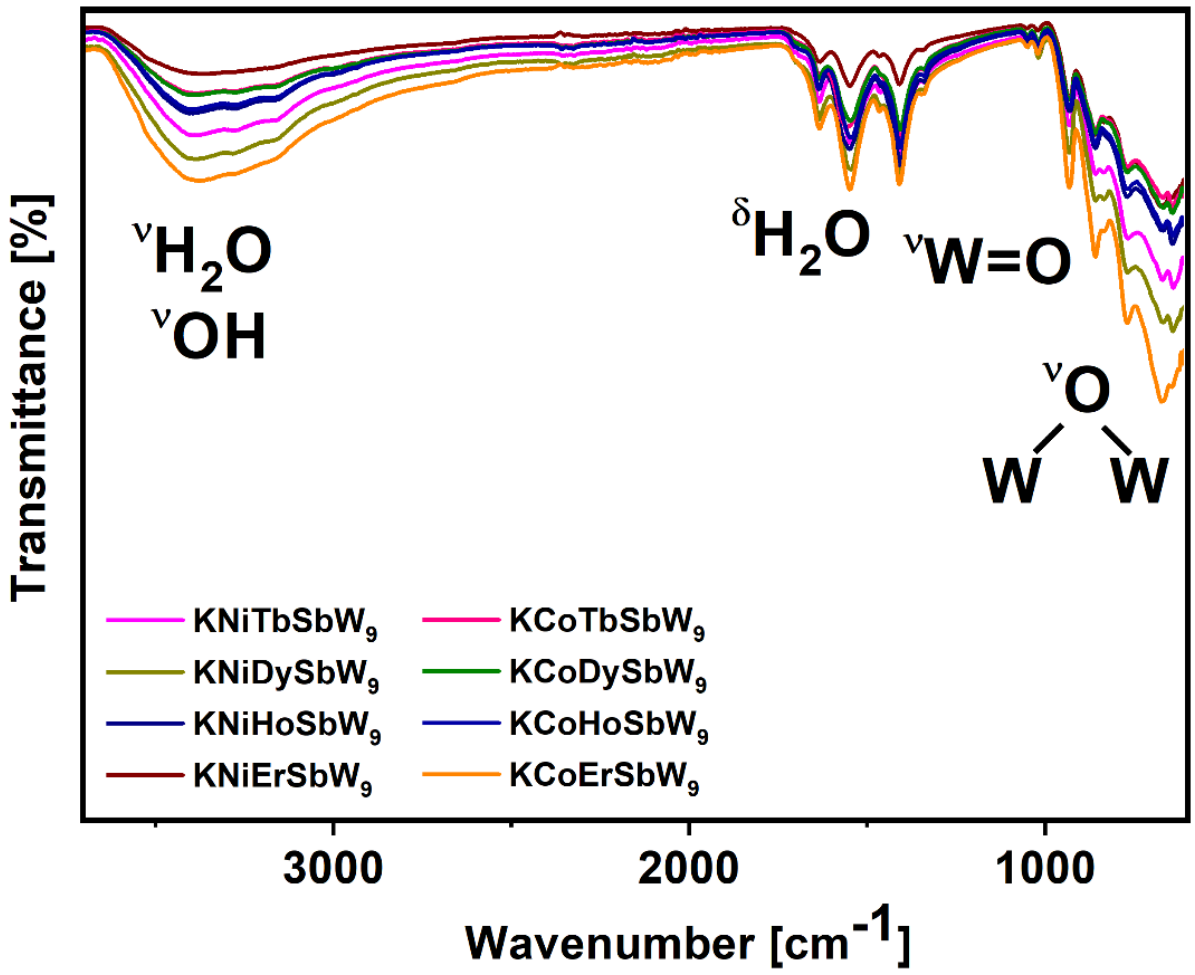

Figure S2. IR-spectra of **KTMLnSbW$_9$**. (ATR-IR, cm^{-1}): 3362.3 (s), 3262.4 (s), 2358.3 (w), 1636.6 (w), 1508.1 (m), 1401.6 (w), 1233.4 (m), 1150.2 (w), 935.3 (w), 934.2 (w) 748.5 (m)

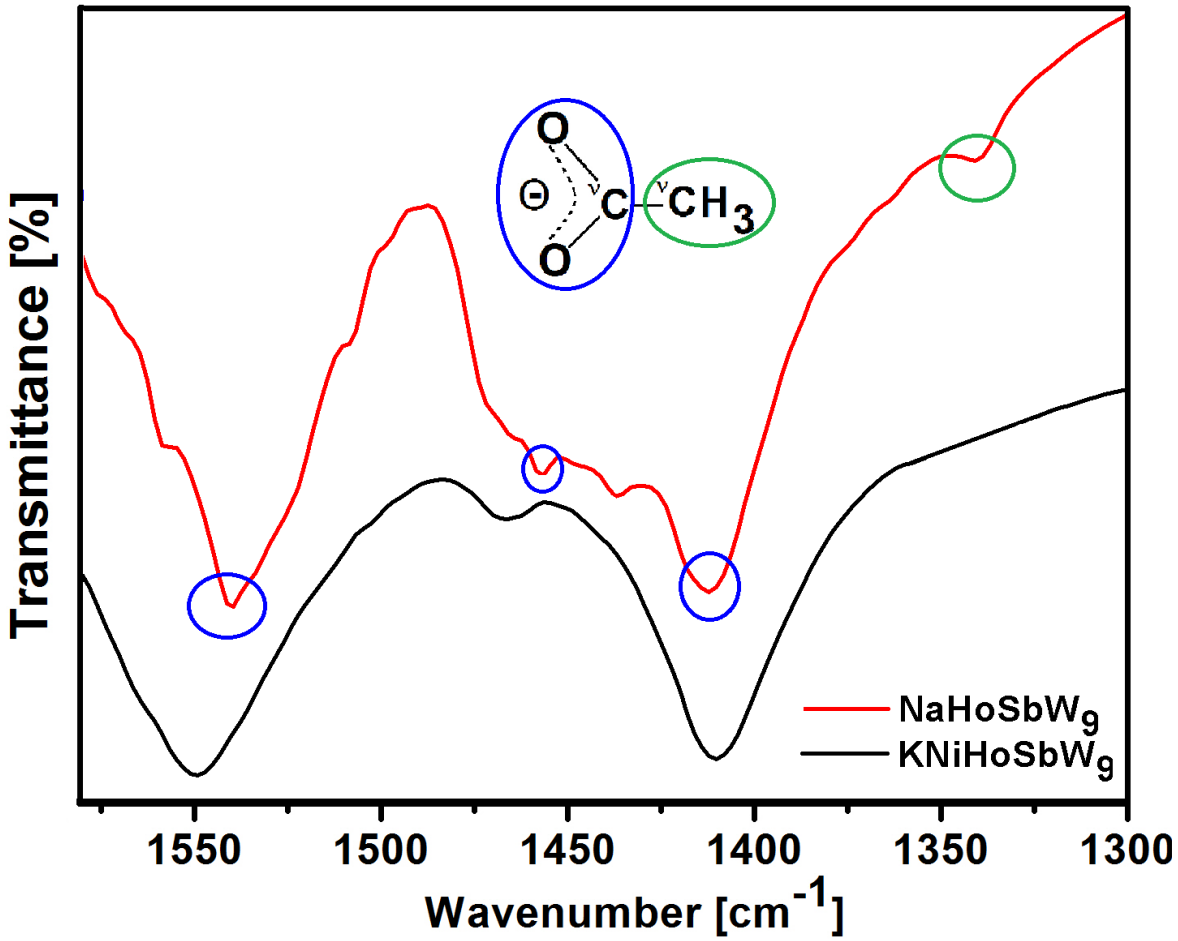

Figure S3. IR-spectrum of **NaHoSbW$_9$** and **KNiHoSbW$_9$** in the range of 1580 – 1300 cm^{-1} showing the bending – and rocking vibrations corresponding to the acetate ligands present in **NaLnSbW$_9$.**

Table S1. Survey of reported crystal structures of 3d-4f heterometallic tungstoantimonates (**TA**). Hpic = picolinic acid, OAc = acetate. Ln = lanthanide, TM = transition metal.

Formula	Type of TA lacunary building block	Number & types of TM centers	Number & types of Ln centers	Ref.
$[Ln(H_2O)_5]_2[TM_4(H_2O)_2(pic)_4(B\text{-}\beta\text{-}SbW_9O_{33})_2]^{4-}$	*B*-β-SbW_9O_{33}	4 Fe^{3+}	4 Pr^{3+}, Nd^{3+}, Sm^{3+}, Eu^{3+}	12
$[TM_2W_4O_9(H_2O)_2(Hpic)_4(B\text{-}\beta\text{-}SbW_9O_{33})_2][Ln(H_2O)_8]_2[TM_4W_2O_7(H_2O)_4(pic)_2(Hpic)_2(B\text{-}\beta\text{-}SbW_9O_{33})_2]^{10-}$	*B*-β-SbW_9O_{33}	6 Fe^{3+}	2 Gd^{3+}, Dy^{3+}	12
$\{[Ln(H_2O)_6]_2[TM_4(H_2O)_2(Hpic)_2(pic)_2(B\text{-}\beta\text{-}SbW_9O_{33})_2]\}_2^{4-}$	*B*-β-SbW_9O_{33}	8 Fe^{3+}	3 Ho^{3+}, Er^{3+}	12
$[Ln_3(H_2O)_5TM(H_2O)_3(Sb_4O_4)(SbW_9O_{33})_3(TMW_6O_{24})(WO_2)_3(CH_3COO)]^{17-}$	*B*-α-SbW_9O_{33}	2 Ni^{2+}	3 La^{3+}, Pr^{3+}, Nd^{3+}	13
$[Ln_3(H_2O)_3TM_3(H_2O)_6(SbW_9O_{33})_3(WO_4)(CO_3)]^{16-}$	*B*-α-SbW_9O_{33}	3 Ni^{2+}	3 La^{3+}, Pr^{3+}, Nd^{3+}	13
$[Ln_3TM_9(\mu_3\text{-}OH)_9(SbW_9O_{33})_2(PW_9O_{34})_3(CH_3COO)_3]^{30-}$	*B*-α-SbW_9O_{33} *B*-α-PW_9O_{34}	9 Ni^{2+}	3 Dy^{3+}, Er^{3+}	13
$[Sb_7W_{36}O_{133}Ln_3TM_2(OAc)(H_2O)_8]^{17-}$	*B*-α-SbW_9O_{33}	2 Ni^{2+}, 2 Zn^{2+}	3 Ce^{3+}	14
$[Sb_7W_{36}O_{133}Ln_3TM_2(OAc)(H_2O)_8]^{17-}$	*B*-α-SbW_9O_{33}	2 Co^{2+}	3 La^{3+}, Pr^{3+}, Nd^{3+}, Sm^{3+}, Eu^{3+}. Gd^{3+}	14
$[Ln(H_2O)_8][Ln(H_2O)_6]\ [TM_4(H_2O)_{10}(B\text{-}\beta\text{-}SbW_9O_{33})_2]\cdot$	*B*-β-SbW_9O_{33}	4 Fe^{3+}	2 Ce^{3+}	15
$[TM(H_2O)Ln_3(H_2O)_5(W_3O_{11})(SbW_9O_{33})_3]^{20-}$	*B*-α-SbW_9O_{33}	1 Co^{2+}, 1 Ni^{2+}	3 Tb^{3+}, Dy^{3+}, Ho^{3+}, Er^{3+}, Y^{3+}	**this work**

Table S2. Full sum formulas of heterometallic **KTMLnSbW$_9$** compounds and the corresponding non-lacunary 4f precursors **NaLnSbW$_9$** (TM = Co^{II}, Ni^{II}; Ln = Tb^{III}, Dy^{III}, Ho^{III}, Er^{III}, Y^{III})

Applied non-lacunary 4f-precursor	***Transition metal source: $CoCl_2$•6H_2O***	***Transition metal source: $NiCl_2$•6H_2O***
$Na_{21}[(Tb(H_2O)(OH)_2(CH_3COO))_3(WO_4)(SbW_9O_{33})_3] \bullet 62\ H_2O$	$K_5Na_{12}H_3[Co(H_2O)Tb_3(H_2O)_5(W_3O_{11})(SbW_9O_{33})_3] \bullet 63\ H_2O$	$K_5Na_{12}H_3[Ni(H_2O)Tb_3(H_2O)_5(W_3O_{11})(SbW_9O_{33})_3] \bullet 94\ H_2O$
$Na_{21}[(Dy(H_2O)(OH)_2(CH_3COO))_3(WO_4)(SbW_9O_{33})_3] \bullet 116\ H_2O$	$K_5Na_{12}H_3[Co(H_2O)Dy_3(H_2O)_5(W_3O_{11})(SbW_9O_{33})_3] \bullet 57\ H_2O$	$K_5Na_{12}H_3[Ni(H_2O)Dy_3(H_2O)_5(W_3O_{11})(SbW_9O_{33})_3] \bullet 110\ H_2O$
$Na_{21}[(Ho(H_2O)(OH)_2(CH_3COO))_3(WO_4)(SbW_9O_{33})_3] \bullet 72\ H_2O$	$K_5Na_{12}H_3[Co(H_2O)Ho_3(H_2O)_5(W_3O_{11})(SbW_9O_{33})_3] \bullet 55\ H_2O$	$K_5Na_{12}H_3[Ni(H_2O)Ho_3(H_2O)_5(W_3O_{11})(SbW_9O_{33})_3] \bullet 81\ H_2O$
$Na_{21}[(Er(H_2O)(OH)_2(CH_3COO))_3(WO_4)(SbW_9O_{33})_3] \bullet 87\ H_2O$	$K_5Na_{12}H_3[Co(H_2O)Er_3(H_2O)_5(W_3O_{11})(SbW_9O_{33})_3] \bullet 64\ H_2O$	$K_5Na_{12}H_3[Ni(H_2O)Er_3(H_2O)_5(W_3O_{11})(SbW_9O_{33})_3] \bullet 63\ H_2O$
$Na_{16}(NH_4)[\{Y(\alpha\text{-}SbW_9O_{31}(OH)_2)(CH_3COO)(H_2O)\}_3(WO_4)]_3\ 48\ H_2O$	$K_5Na_{12}H_3[Co(H_2O)Y_3(H_2O)_5(W_3O_{11})(SbW_9O_{33})_3] \bullet 46\ H_2O$	

Thermogravimetric Analysis

TableS3. TGA data for compounds **$NaLnSbW_9$** • nH_2O (**Fig. S4 – S7**), **$KNiLnSbW_9$** • nH_2O (**Fig. S8 – S11**) and **$KCoLnSbW_9$** • nH_2O (**Fig. S12 – S16**). The discrepancy in the number of weight-loss steps may be observed due to the complex porous structure of POTs. In general, the number of H_2O molecules lost in the region 45-700°C is almost identical with about 50 H_2O molecules.

Compound	Step	T, °C	mass-loss, %	number of molecules corresponding to mass-loss
$[(Tb(H_2O)(OH)_2(CH_3COO))_3(WO_4)(SbW_9O_{33})_3]^{21-}$ • 62 H_2O	I	20-40	0.73	3 H_2O
	II	40-260	10.96	56 H_2O
	III	260-350	2.57	12 H_2O
	IV	350-700	2.47	3 CH_3COO^-
$[(Dy(H_2O)(OH)_2(CH_3COO))_3(WO_4)(SbW_9O_{33})_3]^{21-}$ • 116 H_2O	I	20-40	3.59	17 H_2O
	II	40-300	12.39	65 H_2O
	III	300-450	8.63	43 H_2O
	IV	450-700	2.13	3 CH_3COO^-
$[(Ho(H_2O)(OH)_2(CH_3COO))_3(WO_4)(SbW_9O_{33})_3]^{21-}$ • 72 H_2O	I	25-40	3.31	15.5 H_2O
	II	40-250	8.27	41 H_2O
	III	250-500	5.02	24.5 H_2O
	IV	500-700	2.67	3 CH_3COO^-
$[(Er(H_2O)(OH)_2(CH_3COO))_3(WO_4)(SbW_9O_{33})_3]^{21-}$ • 87 H_2O	I	25-70	3.76	17.5 H_2O
	II	70-340	8.88	44.5 H_2O
	III	240-440	5.81	34 H_2O
	IV	440-700	1.89	3 CH_3COO^-
$[Ni(H_2O)Tb_3(H_2O)_5(W_3O_{11})(SbW_9O_{33})_3]^{20-}$ • 94 H_2O	I	25-44	5.88	29.6 H_2O
	II	44-185	5.16	25.8 H_2O
	III	185-300	2.10	10.2 H_2O
	IV	300-420	3.79	18.7 H_2O
	V	420-700	3.14	15.3 H_2O
$[Ni(H_2O)Dy_3(H_2O)_5(W_3O_{11})(SbW_9O_{33})_3]^{20-}$ • 110	I	20-45	6.18	31 H_2O

H_2O	II	45-200	6.76	34 H_2O
	III	200-430	7.59	39 H_2O
	IV	430-700	2.53	12 H_2O
$[Ni(H_2O)Ho_3(H_2O)_5(W_3O_{11})(SbW_9O_{33})_3]^{20-}$ • 81 H_2O	I	25-40	4.82	24 H_2O
	II	40-300	6.98	35 H_2O
	III	300-475	2.64	13 H_2O
	IV	475-700	2.98	15 H_2O
$[Ni(H_2O)Er_3(H_2O)_5(W_3O_{11})(SbW_9O_{33})_3]^{20-}$ • 63 H_2O	I	20-40	2.75	13 H_2O
	II	40-300	6.63	34 H_2O
	III	300-480	1.97	9 H_2O
	IV	480-700	2.60	13 H_2O
$[Co(H_2O)Tb_3(H_2O)_5(W_3O_{11})(SbW_9O_{33})_3]^{20-}$ • 63 H_2O	I	20-45	1.62	7 H_2O
	II	45-195	5.12	26 H_2O
	III	195-405	5.57	28 H_2O
	IV	405-700	1.58	8 H_2O
$[Co(H_2O)Dy_3(H_2O)_5(W_3O_{11})(SbW_9O_{33})_3]^{20-}$ • 57 H_2O	I	20-45	2.30	11 H_2O
	II	45-210	5.42	27 H_2O
	III	210-445	3.68	18 H_2O
	IV	445-700	1.61	7 H_2O
$[Co(H_2O)Ho_3(H_2O)_5(W_3O_{11})(SbW_9O_{33})_3]^{20-}$ • 55 H_2O	I	20-45	2.36	11.5 H_2O
	II	45-250	5.24	26 H_2O
	III	250-400	2.83	14 H_2O
	IV	400-700	1.87	9.5 H_2O
$[Co(H_2O)Er_3(H_2O)_5(W_3O_{11})(SbW_9O_{33})_3]^{20-}$ • 64 H_2O	I	20-45	2.75	13.5 H_2O
	II	45-320	6.63	34 H_2O
	III	320-480	1.97	9.5 H_2O
	IV	480-700	2.60	13 H_2O
$[Co(H_2O)Y_3(H_2O)_5(W_3O_{11})(SbW_9O_{33})_3]^{20-}$ • 46 H_2O	I	20-50	0.49	2 H_2O
	II	50-700	10.07	50 H_2O

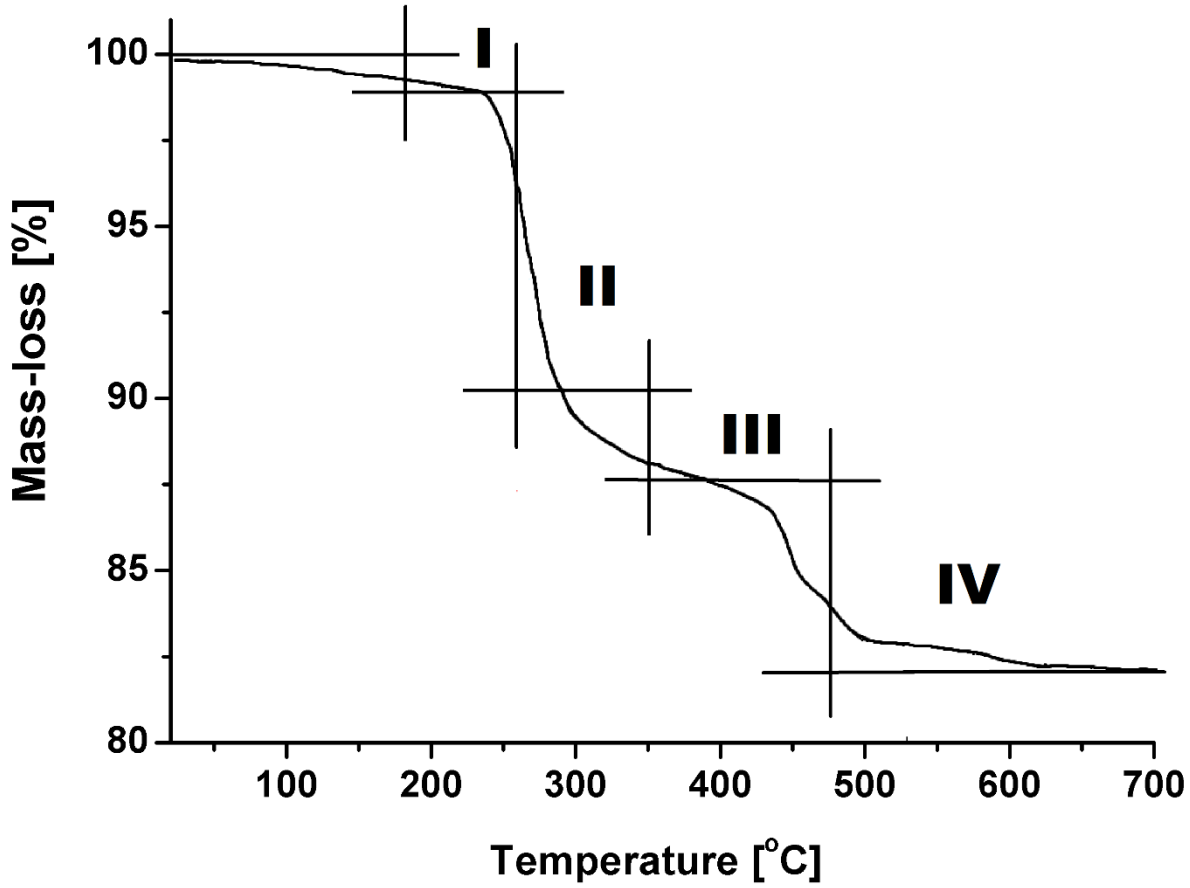

Figure S4. Thermogravimetric curve of **$NaTbSbW_9 \cdot 71\ H_2O$.**

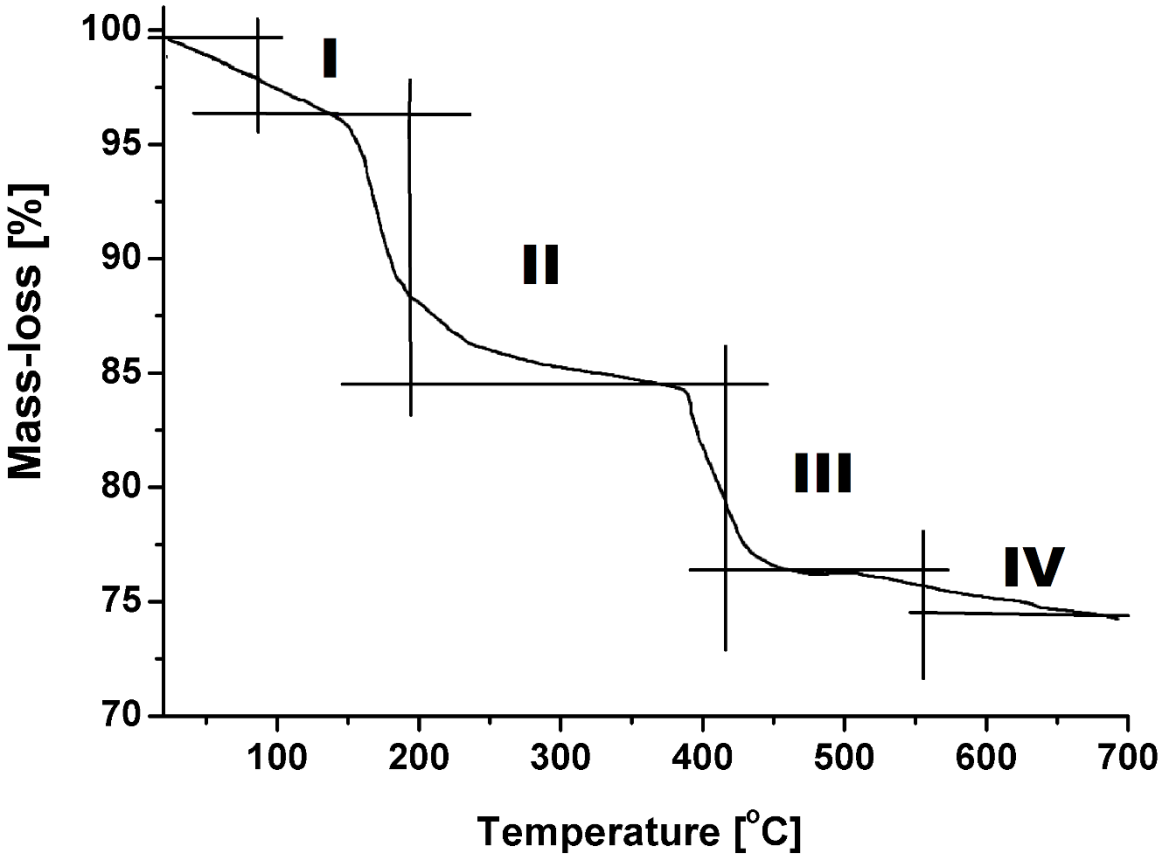

Figure S5. Thermogravimetric curve of **$NaDySbW_9 \cdot 125\ H_2O$.**

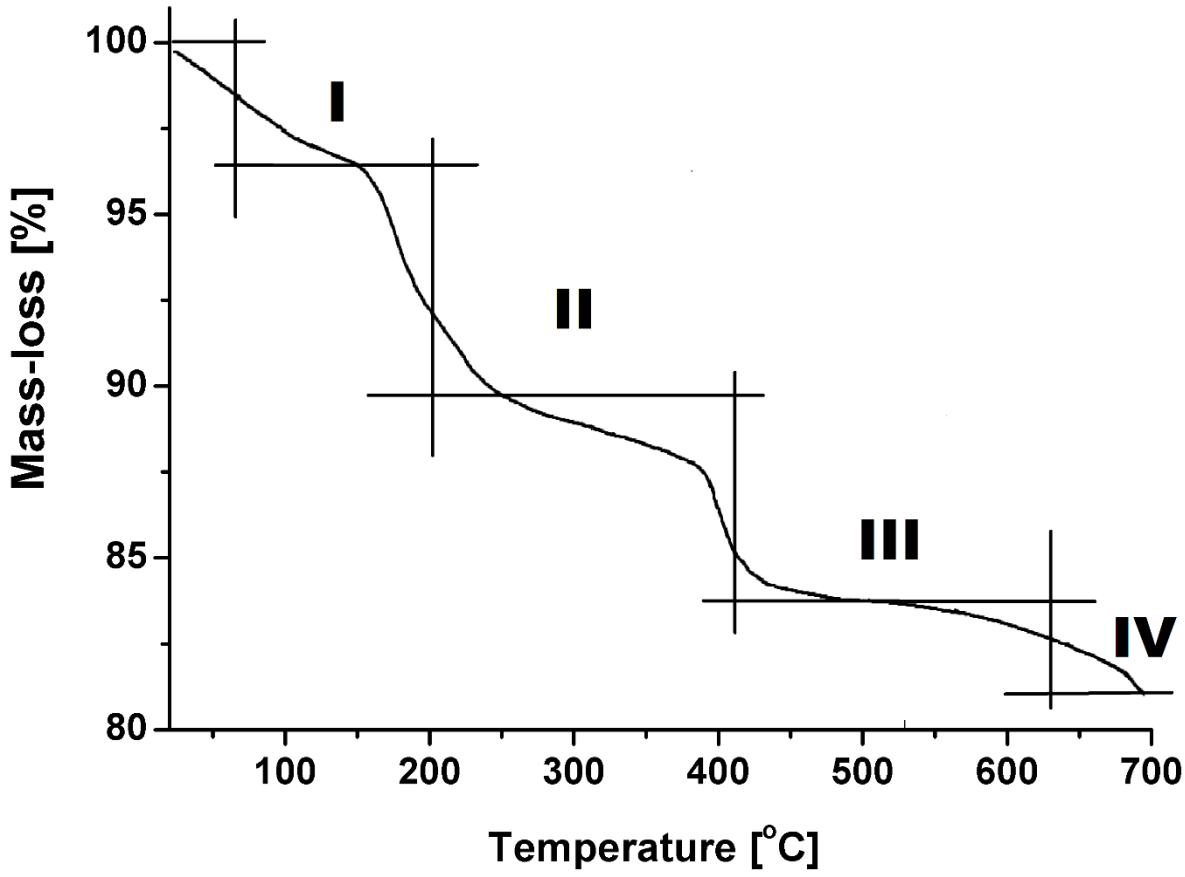

Figure S6. Thermogravimetric curve of **$NaHoSbW_9 \cdot 81\ H_2O$.**

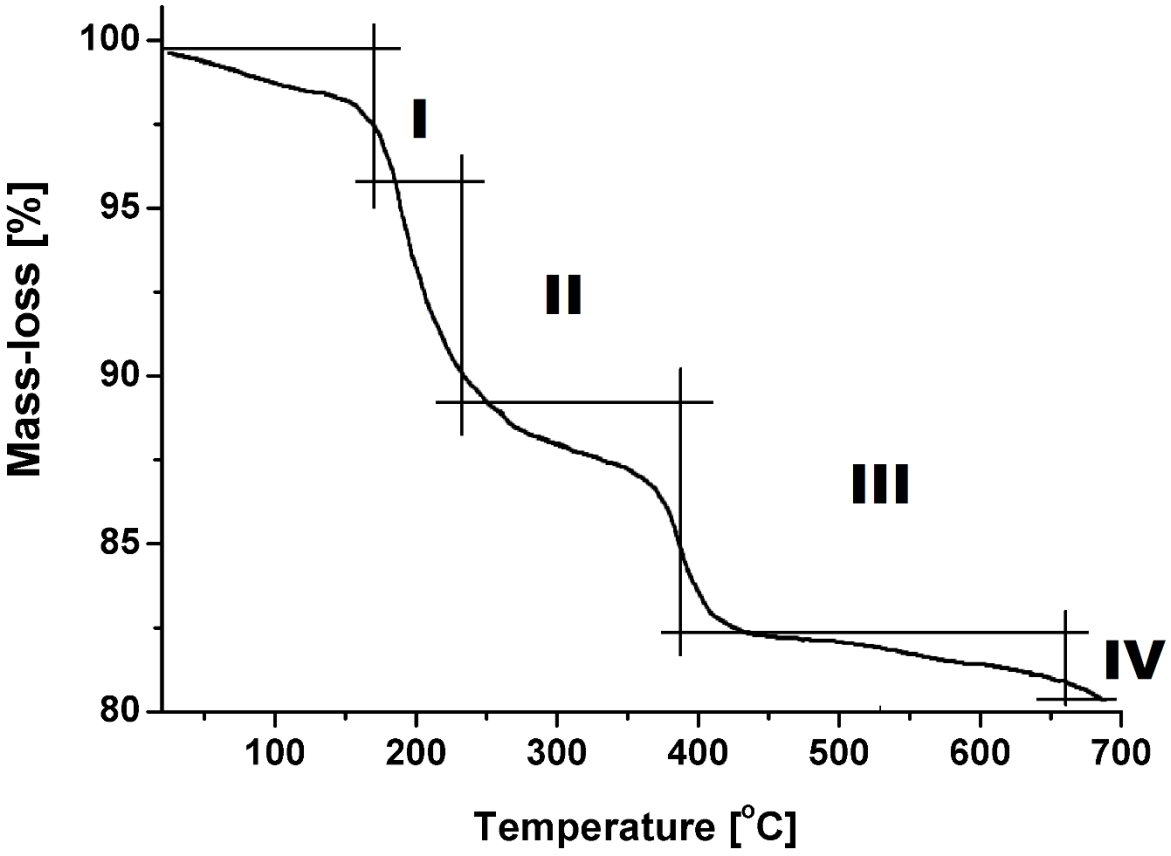

Figure S7. Thermogravimetric curve of **$NaErSbW_9 \cdot 96\ H_2O$.**

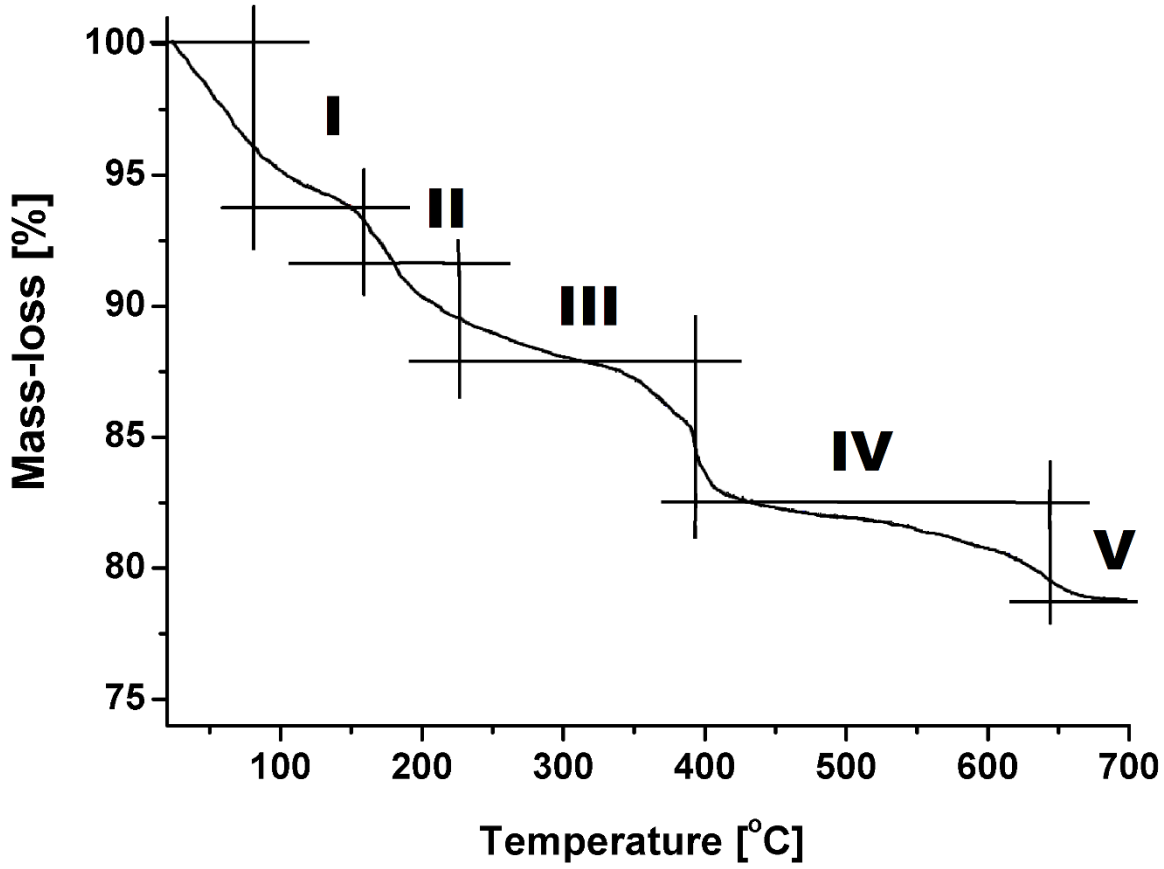

Figure S8. Thermogravimetric curve of **$KNiTbSbW_9 \cdot 100\ H_2O$.**

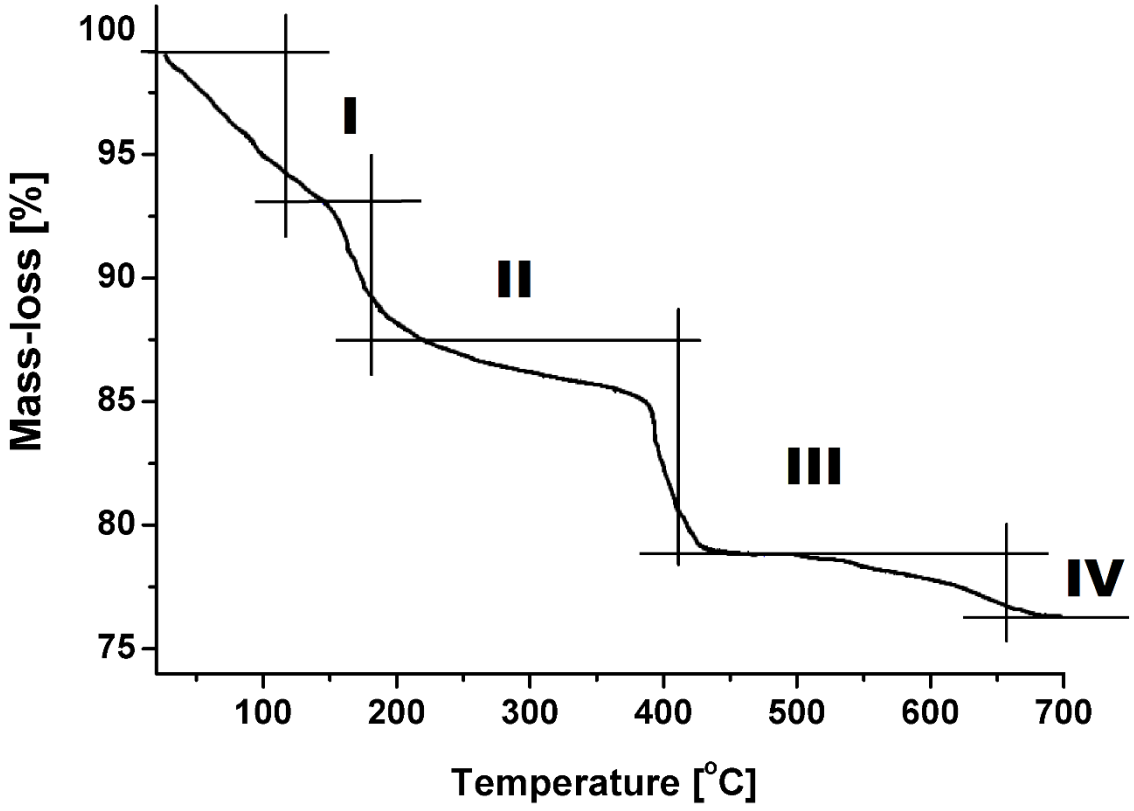

Figure S9. Thermogravimetric curve of **$KNiDySbW_9 \cdot 116\ H_2O$.**

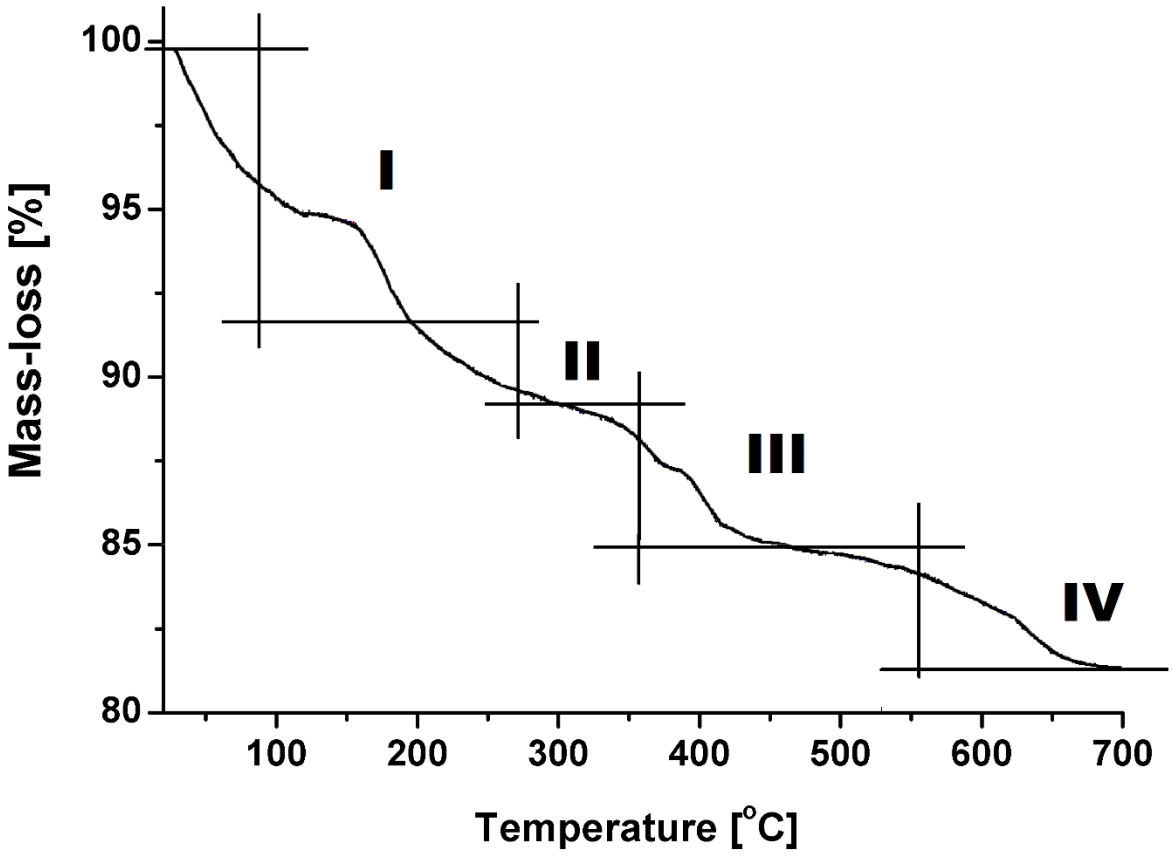

Figure S10. Thermogravimetric curve of **$KNiHoSbW_9 \cdot 87\ H_2O$.**

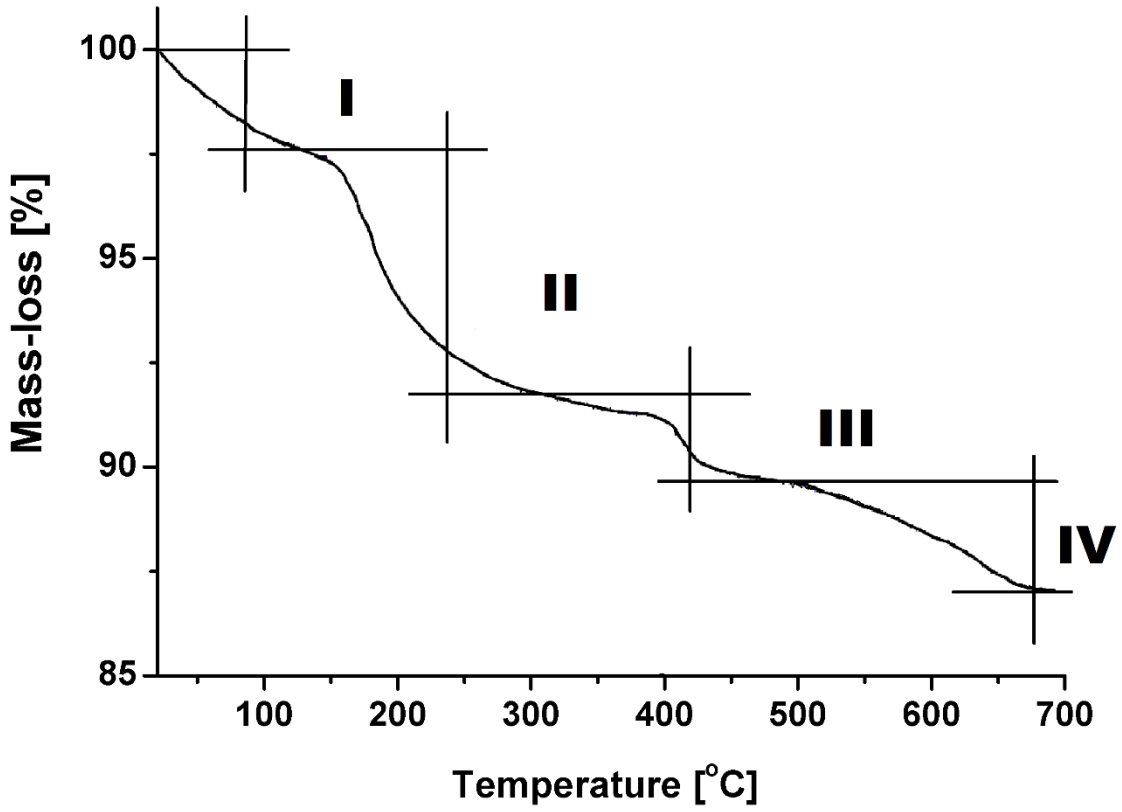

Figure S11. Thermogravimetric curve of **$KNiErSbW_9 \bullet 69\ H_2O$.**

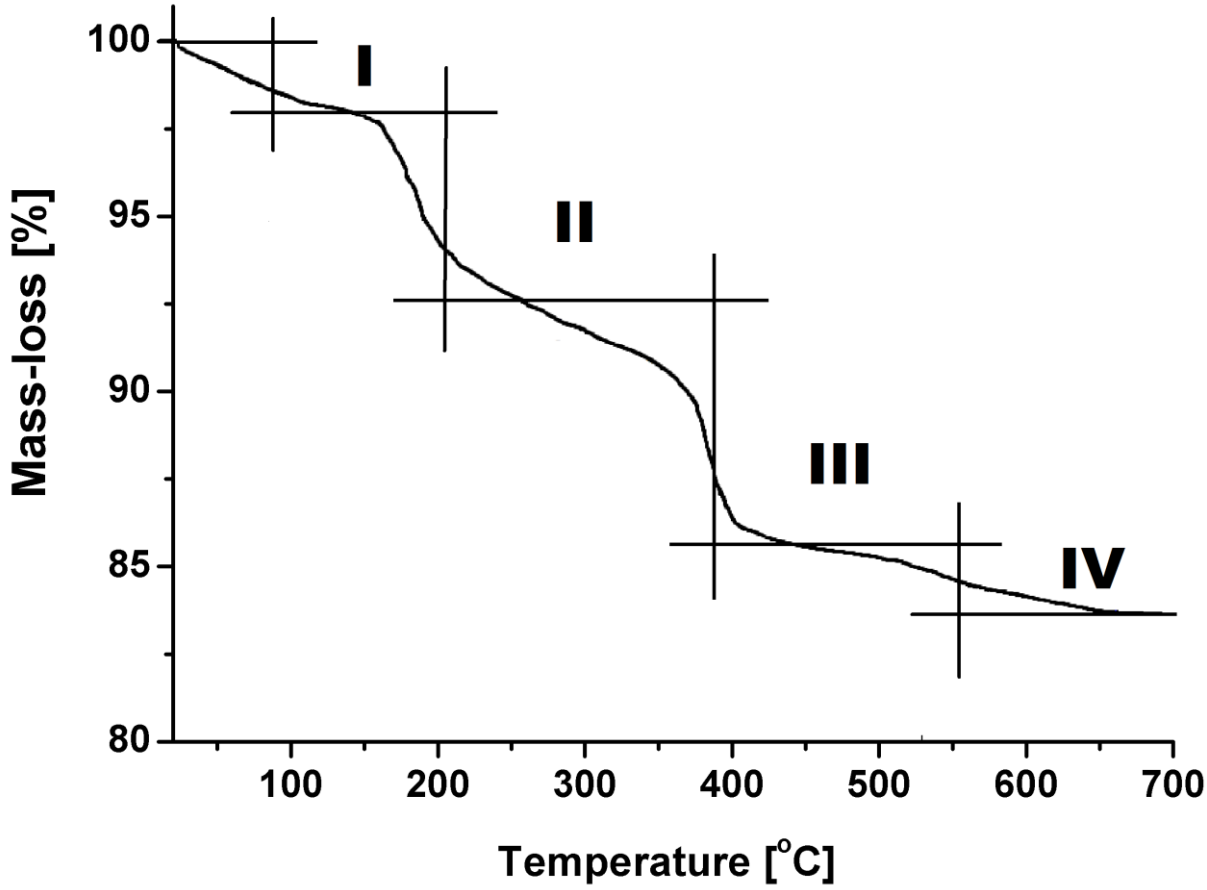

Figure S12. Thermogravimetric curve of **$KCoTbSbW_9 \cdot 69\ H_2O$.**

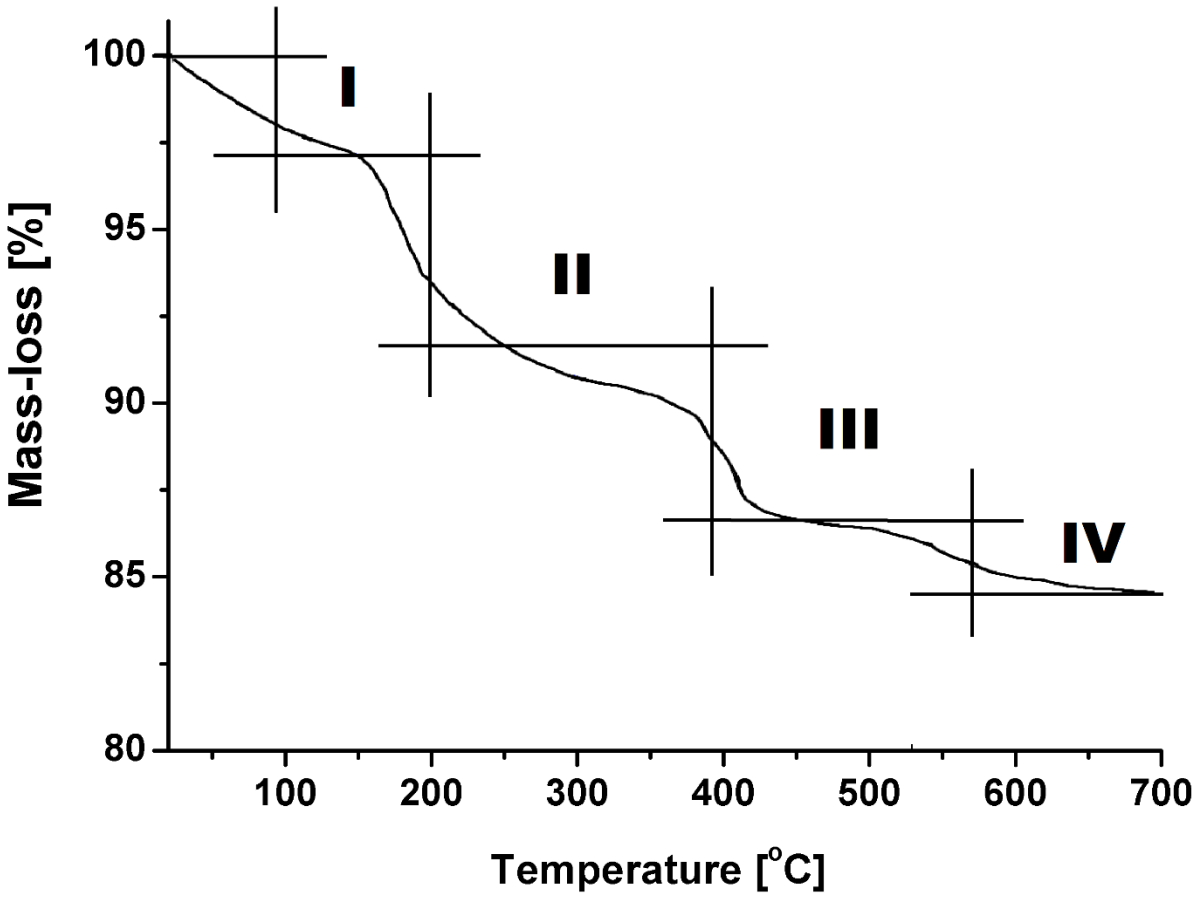

Figure S13. Thermogravimetric curve of **$KCoDySbW_9 \cdot 63\ H_2O$.**

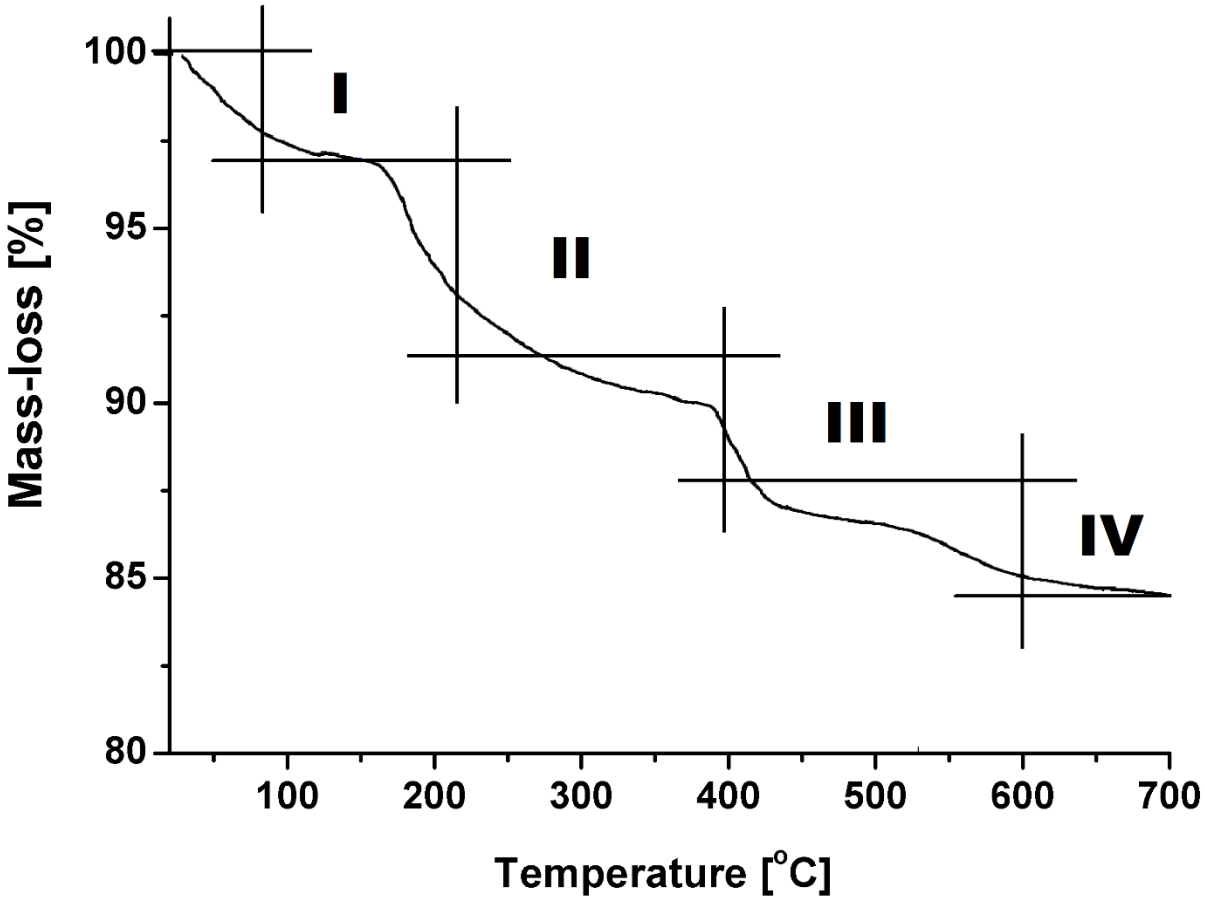

Figure S14. Thermogravimetric curve of **$KCoHoSbW_9 \cdot 61\ H_2O$.**

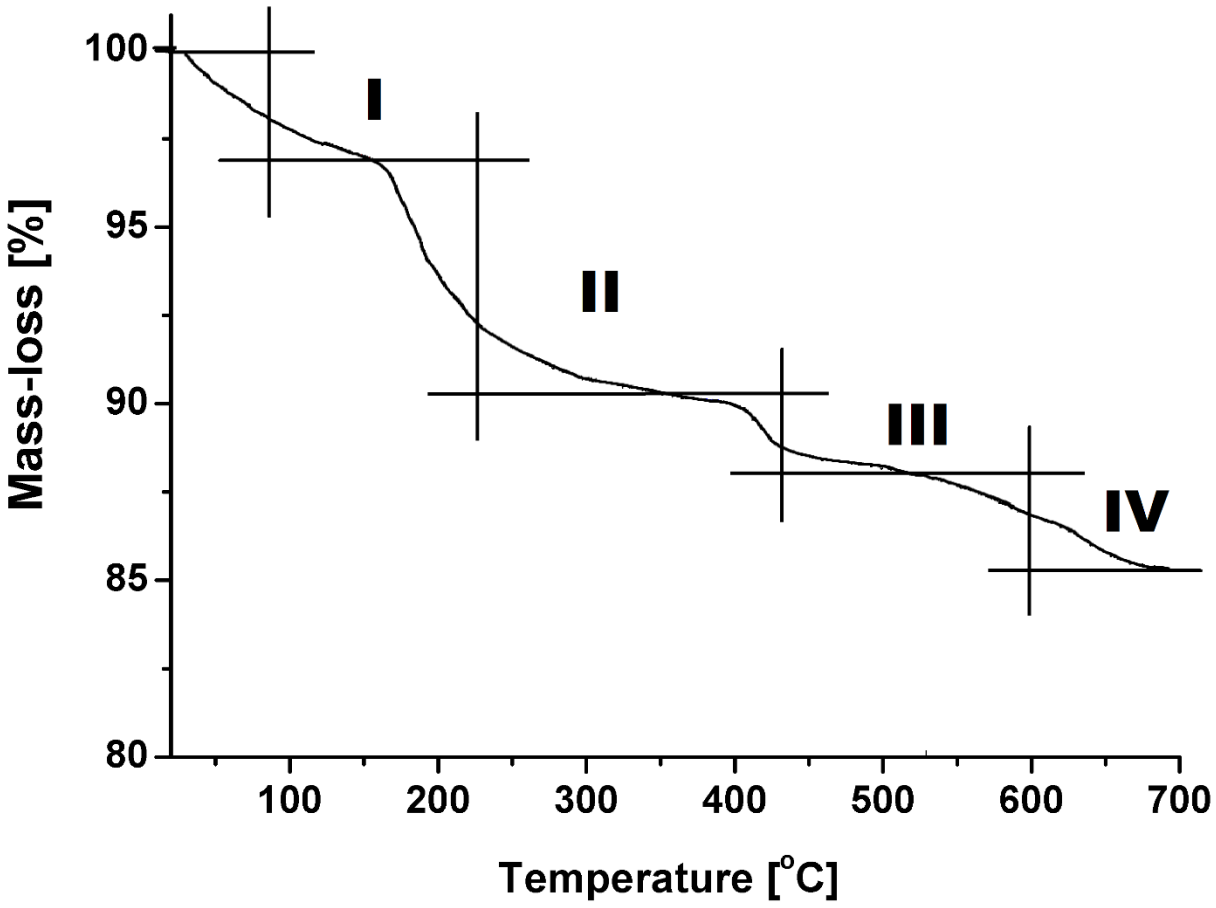

Figure S15. Thermogravimetric curve of **$KCoErSbW_9 \bullet 70\ H_2O$.**

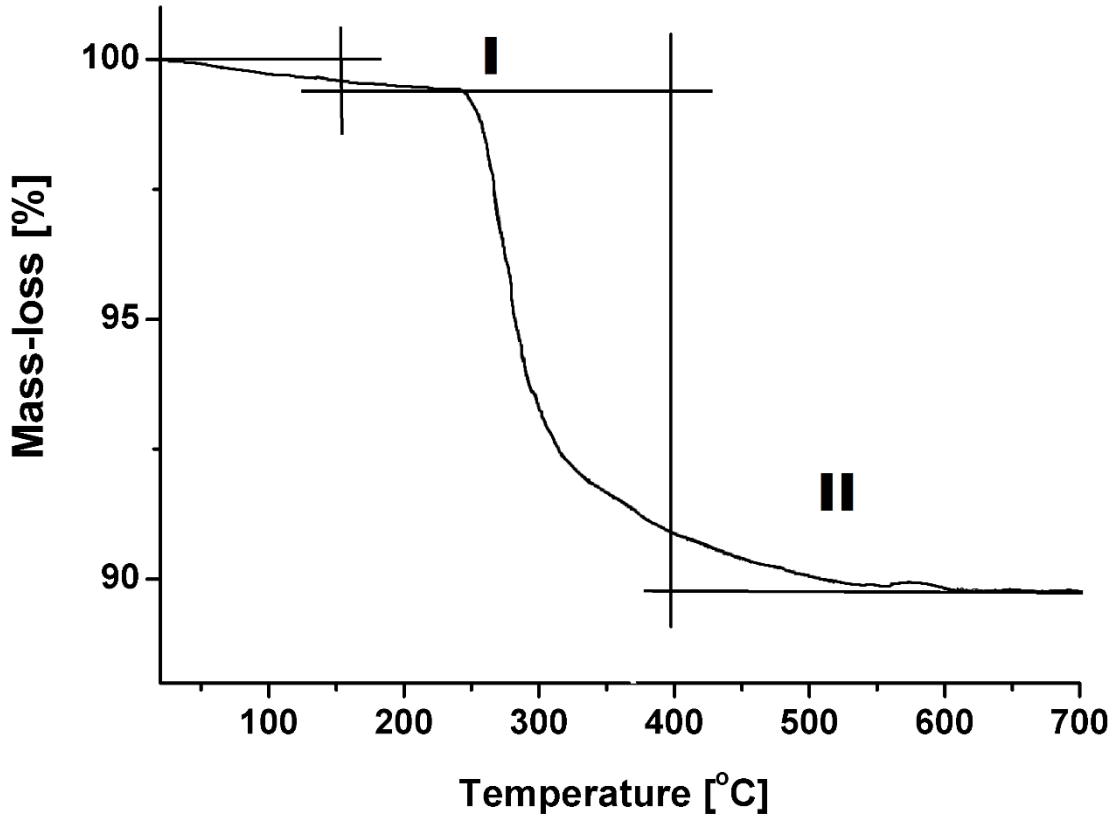

Figure S16. Thermogravimetric curve of **$KCoYSbW_9 \cdot 52\ H_2O$.**

Single-Crystal X-ray Diffraction (SXRD)

Table S4. Experimental parameter and CCDC-Codes. The compounds were measured on a Bruker X8 (**$NaLnSbW_9$**) or on a Bruker D8 (**$KTMLnSbW_9$**) device, respectively. (TM = Co^{II}, Ni^{II}; Ln = Tb^{III}, Dy^{III}, Ho^{III}, Er^{III}, Y^{III}).

Sample	Source	Temp.	Detector Distance	Time/ Frame	#Frames	Frame width	CCDC
		[K]	[mm]	[s]		[°]	
$NaTbSbW_9$	Mo	200	60	25	873	2	1978900
$NaDySbW_9$	Mo	200	40	25	574	2	1978889
$NaHoSbW_9$	Mo	200	40	50	574	2	1978897
$NaErSbW_9$	Mo	200	60	65	862	2	1978896
$KNiTbSbW_9$	Mo	100	40	35	924	0.5	1978895
$KNiDySbW_9$	Mo	100	35	20	2244	0.5	1978894
$KNiErSbW_9$	Mo	100	37	60	1194	0.5	1978899
$KCoTbSbW_9$	Mo	100	50	96	2695	1	1978898

$KCoDySbW_9$	Cu	100	40	15	3963	0.5	1978890
$KCoHoSbW_9$	Mo	100	50	10	896	0.5	1978892
$KCoErSbW_9$	Mo	100	40	20	924	0.5	1978891
$KCoYSbW_9$	Mo	100	37	4	3116	0.3	1978893

Table S5. Sample and crystal data of **$NaTbSbW_9$**

Chemical formula	$C_6H_9Na_{21}O_{147}Sb_3Tb_3W_{28}$	**Crystal system**	trigonal	
Formula weight [g/mol]	8897.82	**Space group**	*R3m*	
Temperature [K]	200.0	**Z**	3	
Measurement method	\f and \w scans	**Volume [Å^3]**	11904.8(13)	
Radiation (Wavelength [Å])	MoKα (λ = 0.71073)	**Unit cell dimensions [Å] and [°]**	30.9094(14)	90.0
Crystal size / [mm^3]	0.15 × 0.15 × 0.075		30.9094(14)	90.0
Crystal habit	clear colorless block		14.3883(9)	120.0
Density (calculated) / [g/cm^3]	3.725	**Absorption coefficient / [mm^{-1}]**	22.179	
Abs. correction Tmin	0.2722	**Abs. correction Tmax**	0.7461	
Abs. correction type	multi-scan	**F(000) [e$^-$]**	11599	

Table S6. Data collection and structure refinement of **$NaTbSbW_9$**

Index ranges	-44 ≤ h ≤ 44, -44 ≤ k ≤ 44, -20 ≤ l ≤ 20	**Theta range for data collection [°]**	3.214 to 61.112	
Reflections number	124243	**Data / restraints / parameters**	8515/37/345	
Refinement method	Least squares	**Final R indices**	all data	R_1 = 0.0699, wR_2 = 0.1019
Function minimized	$\Sigma w(F_o^2 - F_c^2)^2$		I>2σ(I)	R_1 = 0.0425, wR_2 = 0.0880
Goodness-of-fit on F^2	1.074	**Weighting scheme**	$w=1/[\sigma^2(F_o^2)+(0.0546P)^2+622.7385P]$	
Largest diff. peak and hole [e Å^{-3}]	2.17/-2.47		where $P=(F_o^2+2F_c^2)/3$	

Table S7. Sample and crystal data of **$NaDySbW_9$**

Chemical formula	$C_6H_9Dy_3Na_{21}O_{127}Sb_3W_{28}$	**Crystal system**	trigonal
Formula weight [g/mol]	8595.64	**Space group**	*R3m*

Temperature [K]	200.01	**Z**	3	
Measurement method	\f and \w scans	**Volume [Å^3]**	11945.8(19)	
Radiation (Wavelength [Å])	MoKα (λ = 0.71073)	**Unit cell dimensions [Å] and [°]**	30.909(2)	90.0
Crystal size / [mm^3]	0.2 × 0.125 × 0.03		30.909(2)	90.0
Crystal habit	clear colorless block		14.4385(11)	120.0
Density (calculated) / [g/cm^3]	3.317	**Absorption coefficient / [mm^{-1}]**	22.162	
Abs. correction Tmin	0.096	**Abs. correction Tmax**	0.557	
Abs. correction type	multi-scan	**F(000) [e$^-$]**	10191	

Table S8. Data collection and structure refinement of **NaDySbW$_9$**

Index ranges	-42 ≤ h ≤ 44, -44 ≤ k ≤ 44, -20 ≤ l ≤ 20	**Theta range for data collection [°]**	3.204 to 61.052	
Reflections number	100051	**Data / restraints / parameters**	8526/1/242	
Refinement method	Least squares	**Final R indices**	all data	R_1 = 0.0487, wR_2 = 0.0840
Function minimized	Σ $w(F_o^2 - F_c^2)^2$		I>2σ(I)	R_1 = 0.0347, wR_2 = 0.0790
Goodness-of-fit on F²	1.046	**Weighting scheme**	$w=1/[\sigma^2(F_o^2)+(0.0385P)^2+179.3861P]$	
Largest diff. peak and hole [e Å^{-3}]	1.52/-2.09		where $P=(F_o^2+2F_c^2)/3$	

Table S9. Sample and crystal data of **NaHoSbW$_9$**

Chemical formula	$C_6Ho_3Na_{21}O_{164}Sb_3W_{28}$	**Crystal system**	trigonal	
Formula weight [g/mol]	9195.66	**Space group**	*R3m*	
Temperature [K]	200	**Z**	3	
Measurement method	\f and \w scans	**Volume [Å^3]**	11908.9(19)	
Radiation (Wavelength [Å])	MoKα (λ = 0.71073)	**Unit cell dimensions [Å] and [°]**	30.882(2)	90.0
Crystal size / [mm^3]	0.1 × 0. 1 × 0.05		30.882(2)	90.0
Crystal habit	clear pink block		14.4192(11)	120.0
Density (calculated) / [g/cm^3]	3.371	**Absorption coefficient /**	22.261	

		[mm^{-1}]	
Abs. correction Tmin	0.214	**Abs. correction Tmax**	0.402
Abs. correction type	multi-scan	**F(000) [e$^-$]**	10344.0

Table S10. Data collection and structure refinement of **NaHoSbW$_9$**

Index ranges	-37 ≤ h ≤ 37, -37 ≤ k ≤ 37, -17 ≤ l ≤ 17	**Theta range for data collection [°]**	4.154 to 50.688	
Reflections number	81787	**Data / restraints / parameters**	5134/7/258	
Refinement method	Least squares	**Final R indices**	all data	R_1 = 0.0248, wR_2 = 0.0557
Function minimized	Σ w(F_o^2 - F_c^2)^2		I>2σ(I)	R_1 = 0.0223, wR_2 = 0.0543
Goodness-of-fit on F^2	1.051	**Weighting scheme**	w=1/[σ^2(F_o^2)+(0.0240P)^2+321.9862P]	
Largest diff. peak and hole [e Å^{-3}]	2.04/-1.12		where P=(F_o^2+2F_c^2)/3	

Table S11. Sample and crystal data of **NaErSbW$_9$**

Chemical formula	$C_6Er_3Na_{21}O_{155}Sb_3W_{28}$	**Crystal system**	trigonal	
Formula weight [g/mol]	9041.77	**Space group**	*R3m*	
Temperature [K]	200	**Z**	3	
Measurement method	\f and \w scans	**Volume [Å^3]**	11809.9(14)	
Radiation (Wavelength [Å])	MoKα (λ = 0.71073)	**Unit cell dimensions [Å] and [°]**	30.8680(14)	90.0
Crystal size / [mm^3]	0.15 × 0.1 × 0.03		30.8680(14)	90.0
Crystal habit	clear pink block		14.3120(10)	120.0
Density (calculated) / [g/cm^3]	3.422	**Absorption coefficient / [mm^{-1}]**	22.254	
Abs. correction Tmin	0.133	**Abs. correction Tmax**	0.551	
Abs. correction type	multi-scan	**F(000) [e$^-$]**	10425	

Table S12. Data collection and structure refinement of **NaErSbW$_9$**

Index ranges	-39 ≤ h ≤ 39, -39	**Theta range**	4.17 to 54.204

	≤ k ≤ 39, -18 ≤ l ≤ 18	**for data collection [°]**		
Reflections number	92287	**Data / restraints / parameters**	6127/356/243	
Refinement method	Least squares	**Final R indices**	all data	R_1 = 0.0602, wR_2 = 0.1310
Function minimized	$\Sigma w(F_o^2 - F_c^2)^2$		I>2σ(I)	R_1 = 0.0481, wR_2 = 0.1222
Goodness-of-fit on F^2	1.025	**Weighting scheme**	$w=1/[\sigma^2(F_o^2)+(0.0735P)^2+839.4275P]$	
Largest diff. peak and hole [e Å^{-3}]	2.57/-1.65		where $P=(F_o^2+2F_c^2)/3$	

Table S13. Sample and crystal data of **$KNiTbSbW_9$**

Chemical formula	$K_2Na_3NiO_{121}Sb_3Tb_3W_{30}$	**Crystal system**	triclinic	
Formula weight [g/mol]	8499.39	**Space group**	*P-1*	
Temperature [K]	102.06	**Z**	2	
Measurement method	\f and \w scans	**Volume [Å^3]**	7178.6(4)	
Radiation (Wavelength [Å])	MoKα (λ = 0.71073)	**Unit cell dimensions [Å] and [°]**	18.1872(6)	80.9842(11)
Crystal size / [mm^3]	0.08 × 0.06 × 0.04		18.3542(6)	81.2334(10)
Crystal habit	clear green block		24.3503(7)	63.9208(11)
Density (calculated) / [g/cm^3]	3.932	**Absorption coefficient / [mm^{-1}]**	26.217	
Abs. correction Tmin	0.228	**Abs. correction Tmax**	0.42	
Abs. correction type	multi-scan	**F(000) [e$^-$]**	7270	

Table S14. Data collection and structure refinement of **$KNiTbSbW_9$**

Index ranges	-25 ≤ h ≤ 25, -25 ≤ k ≤ 25, -34 ≤ l ≤ 33	**Theta range for data collection [°]**	4.536 to 60.114	
Reflections number	106772	**Data / restraints / parameters**	41889/12/1468	
Refinement method	Least squares	**Final R indices**	all data	R_1 = 0.1096, wR_2 = 0.2014
Function minimized	$\Sigma w(F_o^2 - F_c^2)^2$		I>2σ(I)	R_1 = 0.0740, wR_2 = 0.1725
Goodness-of-fit on F^2	1.047	**Weighting scheme**	$w=1/[\sigma^2(F_o^2)+(0.0604P)^2+301.5323P]$	

Largest diff. peak and hole [e Å^{-3}]	6.44/-5.56		where $P=(F_o^2+2F_c^2)/3$

Table S15. Sample and crystal data of **$KNiDySbW_9$**

Chemical formula	$Dy_3K_4Na_6NiO_{128}Sb_3W_{30}$	**Crystal system**	triclinic	
Formula weight [g/mol]	8769.3	**Space group**	*P-1*	
Temperature [K]	100.5	**Z**	2	
Measurement method	\f and \w scans	**Volume [Å^3]**	7907.3(15)	
Radiation (Wavelength [Å])	MoKα (λ = 0.71073)	**Unit cell dimensions [Å] and [°]**	18.2082(19)	94.753(4)
Crystal size / [mm^3]	0.17 × 0.14 × 0.07		20.315(2)	99.297(3)
Crystal habit	clear green block		24.353(3)	115.475(3)
Density (calculated) / [g/cm^3]	3.683	**Absorption coefficient / [mm^{-1}]**	23.945	
Abs. correction Tmin	0.106	**Abs. correction Tmax**	0.285	
Abs. correction type	multi-scan	**F(000) [e$^-$]**	7530	

Table S16. Data collection and structure refinement of **$KNiDySbW_9$**

Index ranges	-21 ≤ h ≤ 21, -24 ≤ k ≤ 24, -29 ≤ l ≤ 29	**Theta range for data collection [°]**	4.32 to 51.064	
Reflections number	177285	**Data / restraints / parameters**	29152/138/1576	
Refinement method	Least squares	**Final R indices**	all data	R_1 = 0.0942, wR_2 = 0.2262
Function minimized	$\Sigma\, w(F_o^2 - F_c^2)^2$		I>2σ(I)	R_1 = 0.0850, wR_2 = 0.2173
Goodness-of-fit on F^2	1.042	**Weighting scheme**	$w=1/[\sigma^2(F_o^2)+(0.0930P)^2+1011.8275P]$	
Largest diff. peak and hole [e Å^{-3}]	8.44/-3.79		where $P=(F_o^2+2F_c^2)/3$	

Table S17. Sample and crystal data of **$KNiErSbW_9$**

Chemical formula	$Er_3K_2Na_5NiO_{128}Sb_3W_{30}$	**Crystal system**	triclinic
Formula weight [g/mol]	8675.61	**Space group**	*P-1*
Temperature [K]	99.95	**Z**	2
Measurement	\f and \w scans	**Volume [Å^3]**	8022.8(7)

method				
Radiation (Wavelength [Å])	MoKα (λ = 0.71073)	**Unit cell dimensions [Å] and [°]**	18.2734(9)	96.0424(19)
Crystal size / [mm^3]	0.09 × 0.09 × 0.08		20.6197(11)	99.118(2)
Crystal habit	clear green block		24.4271(12)	115.8029(17)
Density (calculated) / [g/cm^3]	3.591	**Absorption coefficient / [mm^{-1}]**	23.716	
Abs. correction Tmin	0.224	**Abs. correction Tmax**	0.253	
Abs. correction type	multi-scan	**F(000) [e$^-$]**	7438	

Table S18. Data collection and structure refinement of **KNiErSbW$_9$**

Index ranges	-22 ≤ h ≤ 21, -24 ≤ k ≤ 24, -27 ≤ l ≤ 29	**Theta range for data collection [°]**	4.468 to 50.7	
Reflections number	128306	**Data / restraints / parameters**	29180/60/1549	
Refinement method	Least squares	**Final R indices**	all data	R_1 = 0.1073, wR_2 = 0.2705
Function minimized	$\Sigma w(F_o^2 - F_c^2)^2$		I>2σ(I)	R_1 = 0.0913, wR_2 = 0.2478
Goodness-of-fit on F^2	1.056	**Weighting scheme**	$w=1/[\sigma^2(F_o^2)+(0.1443P)^2+416.5409P]$	
Largest diff. peak and hole [e Å^{-3}]	6.35/-2.35		where $P=(F_o^2+2F_c^2)/3$	

Table S19. Sample and crystal data of **KCoTbSbW$_9$**

Chemical formula	$CoK_3NaO_{123}Sb_3Tb_3W_{30}$	**Crystal system**	triclinic	
Formula weight [g/mol]	8520.81	**Space group**	*P-1*	
Temperature [K]	100	**Z**	2	
Measurement method	\f and \w scans	**Volume [Å^3]**	7205.1(3)	
Radiation (Wavelength [Å])	MoKα (λ = 0.71073)	**Unit cell dimensions [Å] and [°]**	18.1998(4)	80.6281(7)
Crystal size / [mm^3]	0.11 × 0.1 × 0.05		18.4371(5)	81.3537(7)
Crystal habit	clear pink block		24.3838(6)	63.6381(7)
Density (calculated) / [g/cm^3]	3.928	**Absorption coefficient / [mm^{-1}]**	26.13	
Abs. correction Tmin	0.161	**Abs. correction Tmax**	0.355	

Abs. correction type	multi-scan	**F(000) [e^-]**	7290

Table S20. Data collection and structure refinement of **$KCoTbSbW_9$**

Index ranges	$-21 \le h \le 21$, $-22 \le k \le 22$, $-29 \le l \le 28$	**Theta range for data collection [°]**	4.398 to 50.75	
Reflections number	87744	**Data / restraints / parameters**	26318/1181/1486	
Refinement method	Least squares	**Final R indices**	all data	$R_1 = 0.1334$, $wR_2 = 0.2575$
Function minimized	$\Sigma w(F_o^2 - F_c^2)^2$		$I>2\sigma(I)$	$R_1 = 0.0866$, $wR_2 = 0.2212$
Goodness-of-fit on F^2	1.02	**Weighting scheme**	$w=1/[\sigma^2(F_o^2)+(0.1321P)^2+23.5531P]$	
Largest diff. peak and hole [e $Å^{-3}$]	2.58/-2.17		where $P=(F_o^2+2F_c^2)/3$	

Table S21. Sample and crystal data of **$KCoDySbW_9$**

Chemical formula	$CoDy_3K_3Na_8O_{121}Sb_3W_{30}$	**Crystal system**	triclinic	
Formula weight [g/mol]	8664.4	**Space group**	*P-1*	
Temperature [K]	100	**Z**	2	
Measurement method	\f and \w scans	**Volume [$Å^3$]**	7752.4(14)	
Radiation (Wavelength [Å])	CuKα (λ = 1.54178)	**Unit cell dimensions [Å] and [°]**	18.2885(16)	93.201(6)
Crystal size / [mm^3]	0.12 × 0.12 × 0.04		19.955(2)	99.171(4)
Crystal habit	clear pink block		24.429(2)	117.082(4)
Density (calculated) / [g/cm^3]	3.712	**Absorption coefficient / [mm^{-1}]**	54.05	
Abs. correction Tmin	0.0122	**Abs. correction Tmax**	0.1099	
Abs. correction type	multi-scan	**F(000) [e^-]**	7422	

Table S22. Data collection and structure refinement of **$KCoDySbW_9$**

Index ranges	$-21 \le h \le 21$, $-23 \le k \le 23$, $-28 \le l \le 21$	**Theta range for data collection [°]**	5.028 to 127.374	
Reflections number	89327	**Data / restraints / parameters**	25114/6/1522	
Refinement	Least squares	**Final R**	all data	$R_1 = 0.0679$, $wR_2 =$

method		**indices**		0.1795
Function minimized	$\Sigma w(F_o^2 - F_c^2)^2$		I>2σ(I)	R_1 = 0.0628, wR_2 = 0.1739
Goodness-of-fit on F^2	1.096	**Weighting scheme**	w=1/[$\sigma^2(F_o^2)$+(0.0901P)^2+66.3364P]	
Largest diff. peak and hole [e Å^{-3}]	4.93/-1.48		where P=(F_o^2+2F_c^2)/3	

Table S23. Sample and crystal data of **$KCoHoSbW_9$**

Chemical formula	$CoHo_3K_3Na_4O_{120}Sb_3W_{30}$	**Crystal system**	triclinic	
Formula weight [g/mol]	8555.97	**Space group**	*P-1*	
Temperature [K]	100	**Z**	2	
Measurement method	\f and \w scans	**Volume [Å^3]**	7648.6(10)	
Radiation (Wavelength [Å])	MoKα (λ = 0.71073)	**Unit cell dimensions [Å] and [°]**	18.2065(13)	79.311(2)
Crystal size / [mm^3]	0.22 × 0.18 × 0.1		19.7028(15)	81.003(2)
Crystal habit	clear pink block		24.4697(19)	62.841(2)
Density (calculated) / [g/cm^3]	3.715	**Absorption coefficient / [mm^{-1}]**	24.786	
Abs. correction Tmin	0.003	**Abs. correction Tmax**	0.0186	
Abs. correction type	multi-scan	**F(000) [e$^-$]**	7316	

Table S24. Data collection and structure refinement of **$KCoHoSbW_9$**

Index ranges	-21 ≤ h ≤ 21, -21 ≤ k ≤ 23, -29 ≤ l ≤ 28	**Theta range for data collection [°]**	4.372 to 50.892	
Reflections number	58599	**Data / restraints / parameters**	27828/84/1468	
Refinement method	Least squares	**Final R indices**	all data	R_1 = 0.0920, wR_2 = 0.2213
Function minimized	$\Sigma w(F_o^2 - F_c^2)^2$		I>2σ(I)	R_1 = 0.0753, wR_2 = 0.2073
Goodness-of-fit on F^2	1.041	**Weighting scheme**	w=1/[$\sigma^2(F_o^2)$+(0.1135P)^2+295.0967P]	
Largest diff. peak and hole [e Å^{-3}]	7.17/-3.23		where P=(F_o^2+2F_c^2)/3	

Table S25. Sample and crystal data of **$KCoErSbW_9$**

Chemical formula	$CoEr_3K_5Na_{12}O_{110}Sb_3W_{30}$	**Crystal system**	triclinic	
Formula weight [g/mol]	8672.84	**Space group**	*P-1*	
Temperature [K]	101.77	**Z**	2	
Measurement method	\f and \w scans	**Volume [Å^3]**	7788.5(7)	
Radiation (Wavelength [Å])	MoKα (λ = 0.71073)	**Unit cell dimensions [Å] and [°]**	18.3211(9)	94.6511(17)
Crystal size / [mm^3]	0.12 × 0.08 × 0.06		19.9321(10)	99.2600(15)
Crystal habit	clear pink block		24.6926(13)	117.2426(13)
Density (calculated) / [g/cm^3]	3.698	**Absorption coefficient / [mm^{-1}]**	24.503	
Abs. correction Tmin	0.018	**Abs. correction Tmax**	0.0504	
Abs. correction type	multi-scan	**F(000) [e$^-$]**	7422	

Table S26. Data collection and structure refinement of **$KCoErSbW_9$**

Index ranges	-25 ≤ h ≤ 25, -28 ≤ k ≤ 28, -34 ≤ l ≤ 34	**Theta range for data collection [°]**	4.09 to 60.128	
Reflections number	116105	**Data / restraints / parameters**	45386/0/1738	
Refinement method	Least squares	**Final R indices**	all data	R_1 = 0.0453, wR_2 = 0.0971
Function minimized	Σ $w(F_o^2 - F_c^2)^2$		I>2σ(I)	R_1 = 0.0390, wR_2 = 0.0940
Goodness-of-fit on F²	1.054	**Weighting scheme**	$w=1/[\sigma^2(F_o^2)+(0.0357P)^2+163.9879P]$	
Largest diff. peak and hole [e Å^{-3}]	6.64/-5.01		where $P=(F_o^2+2F_c^2)/3$	

Table S27. Sample and crystal data of **$KCoYSbW_9$**

Chemical formula	$CoK_4Na_8O_{127}Sb_3W_{30}Y_3$	**Crystal system**	triclinic	
Formula weight [g/mol]	8579.23	**Space group**	*P-1*	
Temperature [K]	100	**Z**	2	
Measurement method	\f and \w scans	**Volume [Å^3]**	7982.1(14)	
Radiation (Wavelength [Å])	MoKα (λ = 0.71073)	**Unit cell dimensions [Å] and [°]**	18.2516(18)	94.866(4)
Crystal size / [mm^3]	0.12 × 0.12 × 0.05		20.402(2)	99.426(4)

Crystal habit	clear pink block		24.473(2)	115.603(4)
Density (calculated) / [g/cm^3]	3.57	**Absorption coefficient / [mm^{-1}]**	23.403	
Abs. correction Tmin	0.2675	**Abs. correction Tmax**	0.7461	
Abs. correction type	multi-scan	**F(000) [e$^-$]**	7395	

Table S28. Data collection and structure refinement of **$KCoYSbW_9$**

Index ranges	-23 ≤ h ≤ 23, -26 ≤ k ≤ 26, -31 ≤ l ≤ 31	**Theta range for data collection [°]**	4.04 to 54.968	
Reflections number	225113	**Data / restraints / parameters**	36563/3393/1518	
Refinement method	Least squares	**Final R indices**	all data	R_1 = 0.1229, wR_2 = 0.2146
Function minimized	$\Sigma w(F_o^2 - F_c^2)^2$		I>2σ(I)	R_1 = 0.0749, wR_2 = 0.1848
Goodness-of-fit on F²	1.054	**Weighting scheme**	$w=1/[\sigma^2(F_o^2)+(0.0990P)^2+247.5574P]$	
Largest diff. peak and hole [e Å^{-3}]	7.18/-4.23		where $P=(F_o^2+2F_c^2)/3$	

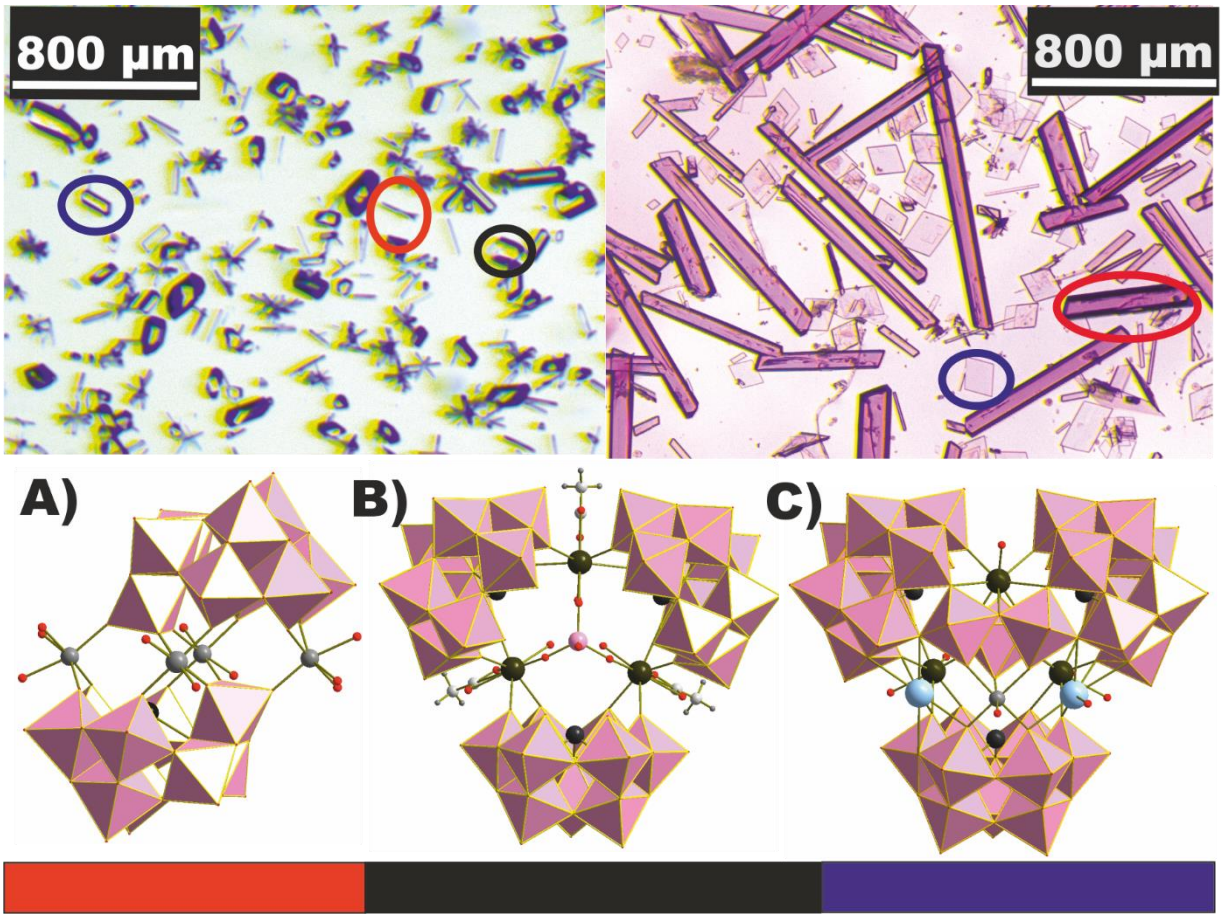

Figure S17. Microscopic images of mixed crystal phases of **A)** Krebs-type POM $Na_{10}[(TM(H_2O)_3)_2(WO_2)_2(SbW_9O_{33})_2]$ (red circled crystal), **B)** unreacted 4f-precursor $Na_{21}[(Ln(H_2O)(OH)_2(CH_3COO))_3(WO_4)(SbW_9O_{33})_3]$ (black circled crystal) and **C)** the corresponding 3d-4f compound $K_5Na_{12}H_3[TM(H_2O)Ln_3(H_2O)_5(W_3O_{11})(SbW_9O_{33})_3]$ (TM = Co^{II}, Ni^{II}; Ln = Tb^{III}, Dy^{III}, Ho^{III}, Er^{III}, Y^{III}) (violet circled crystal) before changing the K^+ content of the reaction mixture. Color legend: WO_6, fairy floss octahedra; Ln^{III}, black balls; TM^{II}, grey balls; Sb^{III}, dark green balls; K^+, light blue balls; O, red balls; C, white balls, tetrahedrally coordinated WO_4 capping unit, pink ball.

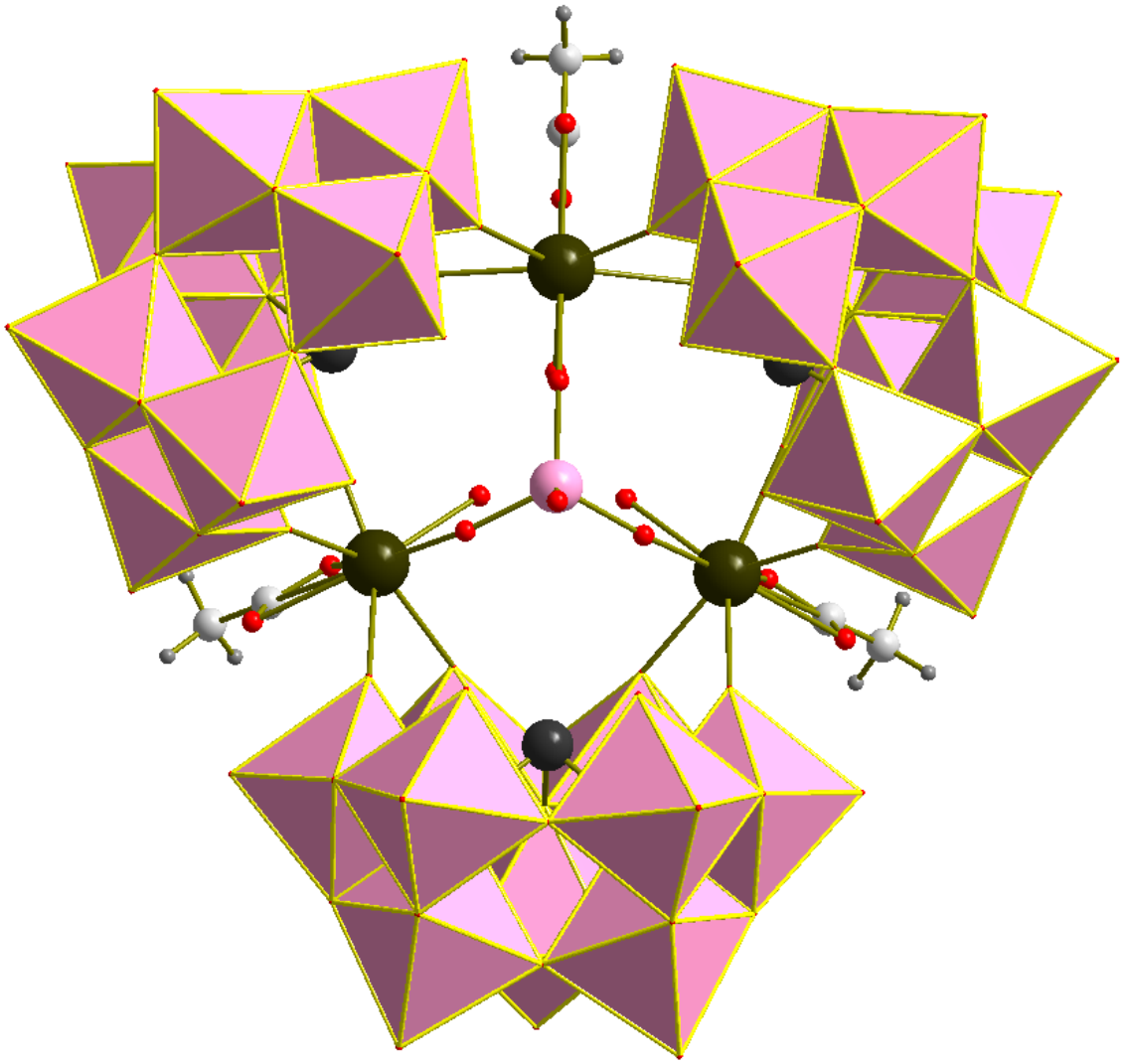

Figure S18. Crystal structure of **NaLnSbW$_9$** (Ln = Tb^{III}, Dy^{III}, Ho^{III}, Er^{III}). Color legend: WO_6, fairy floss octahedra; Ln^{III}, dark green balls; Sb^{III}, dark grey balls; O, red balls; C, white balls; tetrahedrally coordinated WO_4 capping unit, fairy floss (pink) ball.

Powder X-ray Diffraction (PXRD)

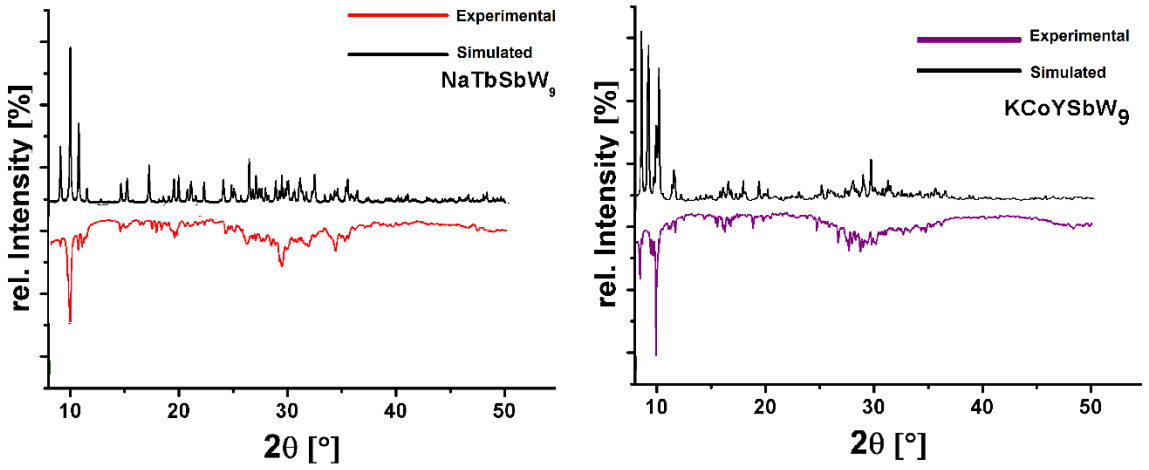

Figure S19. Comparison of the experimental and simulated PXRD patterns of **NaTbSbW$_9$** and **KCoYSbW$_9$**.

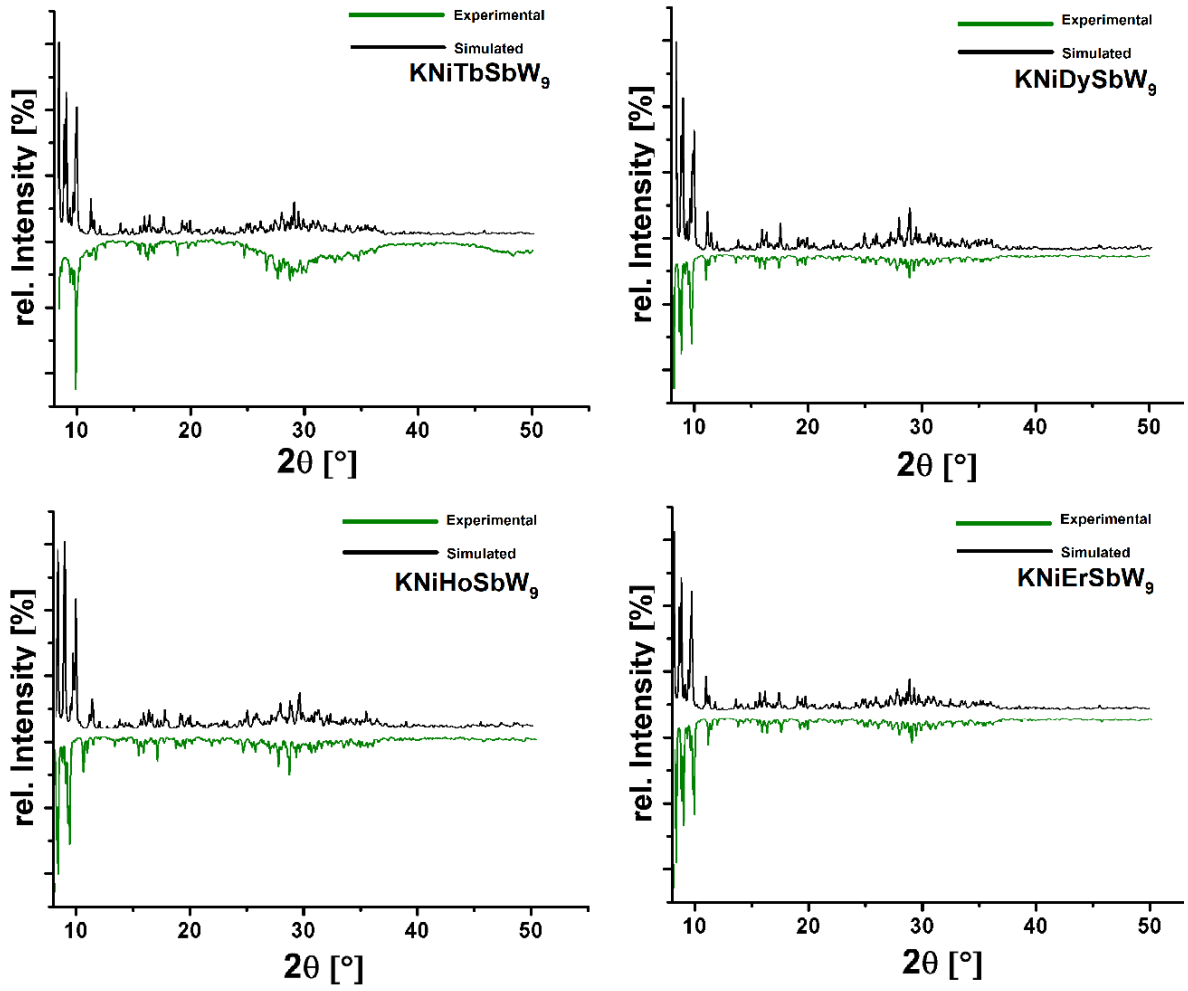

Figure S20. Comparison of the experimental and simulated PXRD patterns of **KNiLnSbW$_9$** (Ln = Tb^{III}, Dy^{III}, Ho^{III}, Er^{III}).

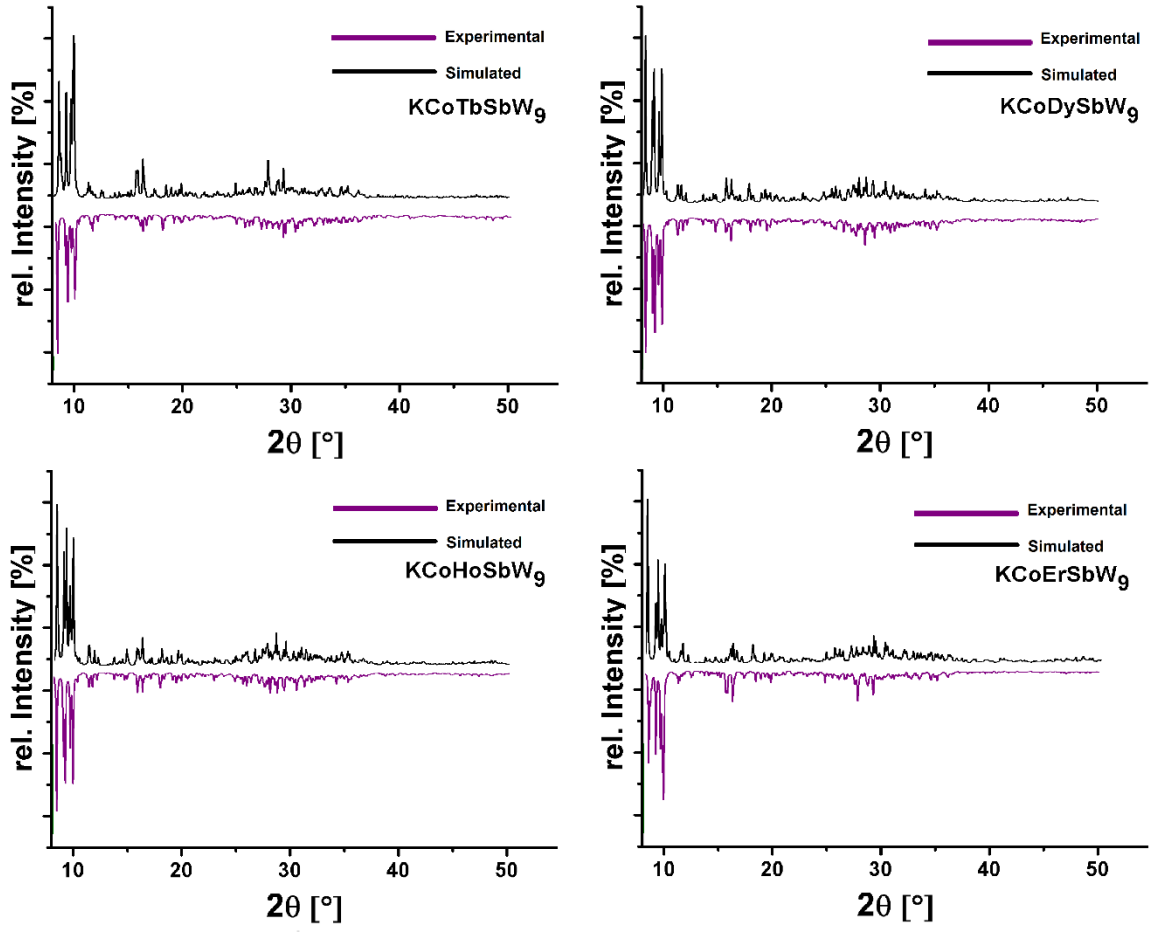

Figure S21. Comparison of the experimental and simulated PXRD patterns of **KCoLnSbW$_9$** (Ln = Tb^{III}, Dy^{III}, Ho^{III}, Er^{III}).

UV/Vis Spectroscopy

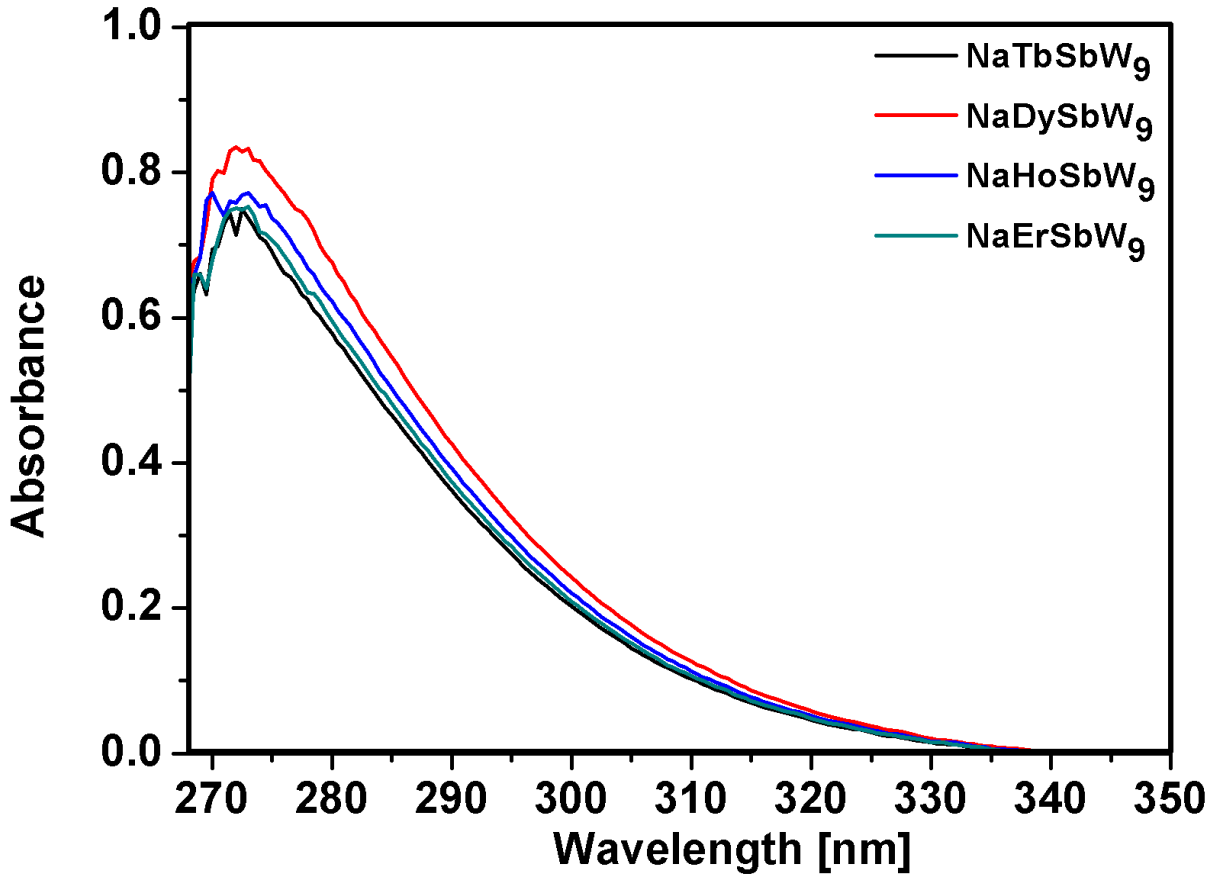

Figure S22. UV/Vis-spectrum of the **NaLnSbW$_9$** (Ln = Tb^{III}, Dy^{III}, Ho^{III}, Er^{III}) 4f-precursors showing typical O→W ligand−to−metal charge−transfer (274 nm).

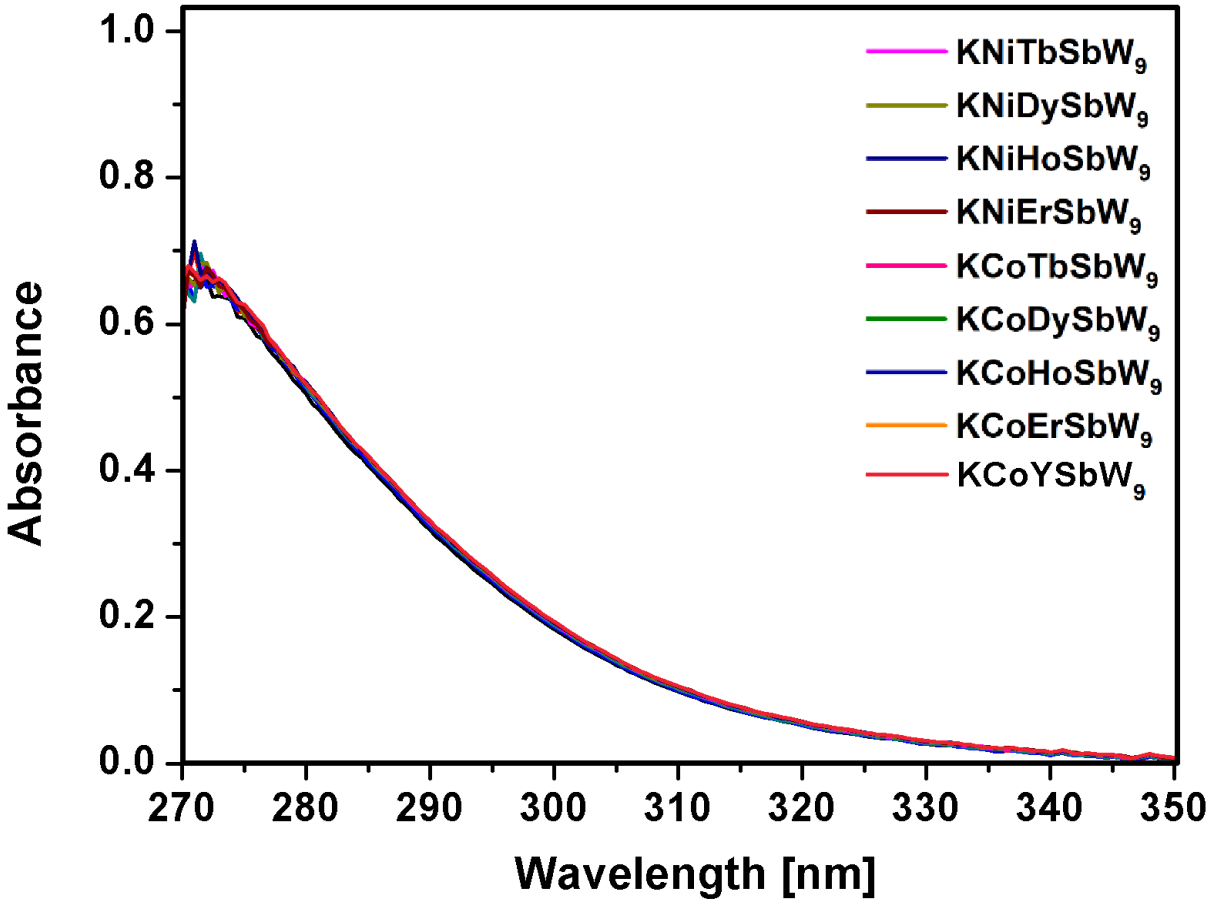

Figure S23. UV/Vis-spectrum of **KTMLnSbW$_9$** (TM = Ni^{II}, Co^{II}; Ln = Tb^{III}, Dy^{III}, Ho^{III}, Er^{III}) showing typical O→W ligand−to−metal charge−transfer (272 nm).

Magnetism

The extracted temperature and field dependence of relaxation times in **KCoDySbW$_9$**, **KNiDySbW$_9$** and **KCoYSbW$_9$** can be analyzed based on four relaxation mechanisms given by equation:

$$\tau_{T/H}^{-1}(T,H) = \frac{Q_1}{1+Q_2H^2} + \tau_0^{-1} * \exp\left(-\frac{U_{eff}}{kT}\right) + AH^4T + CT^n \quad \textbf{(eq-S1)}$$

Here, the first term represents Quantum Tunneling of Magnetization (QTM), the second term is Orbach, third is a Direct and the last term is the Raman process. H represents the applied magnetic field, and T is the temperature. In order to constrain the variable parameters and to avoid overparameterization, the temperature and field dependence of relaxation times was fitted simultaneously[16] (**Fig. S27, S28**) (vector of data: τ^{-1} in s^{-1}, T in Kelvin and H in kOe).

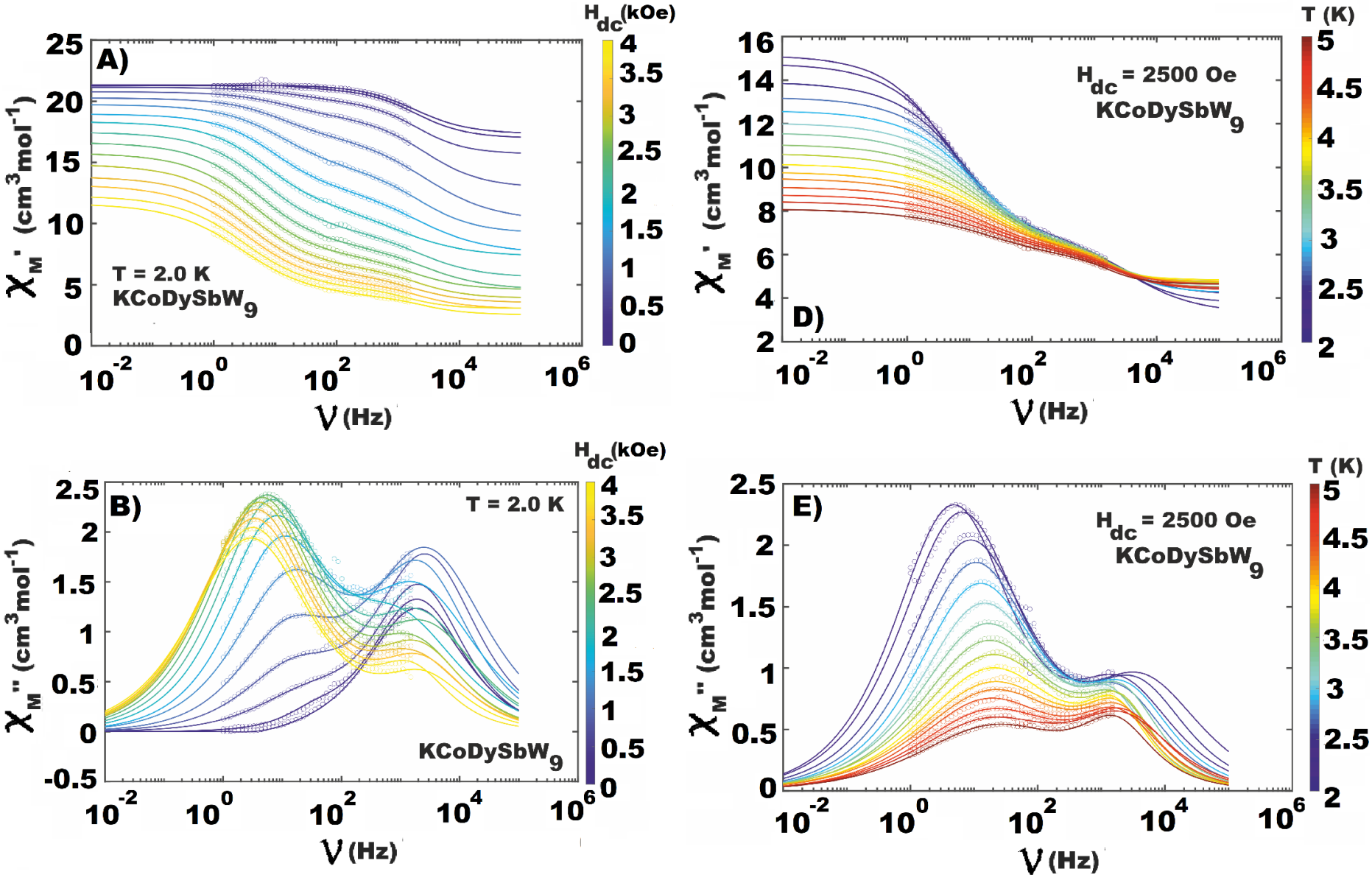
A)
T = 2.0 K
KCoDySbW9
χM' (cm3mol-1)
ν (Hz)
Hdc(kOe)
B)
T = 2.0 K
KCoDySbW9
χM'' (cm3mol-1)
ν (Hz)
Hdc(kOe)
D)
Hdc = 2500 Oe
KCoDySbW9
χM' (cm3mol-1)
ν (Hz)
T (K)
E)
Hdc = 2500 Oe
KCoDySbW9
χM'' (cm3mol-1)
ν (Hz)
T (K)

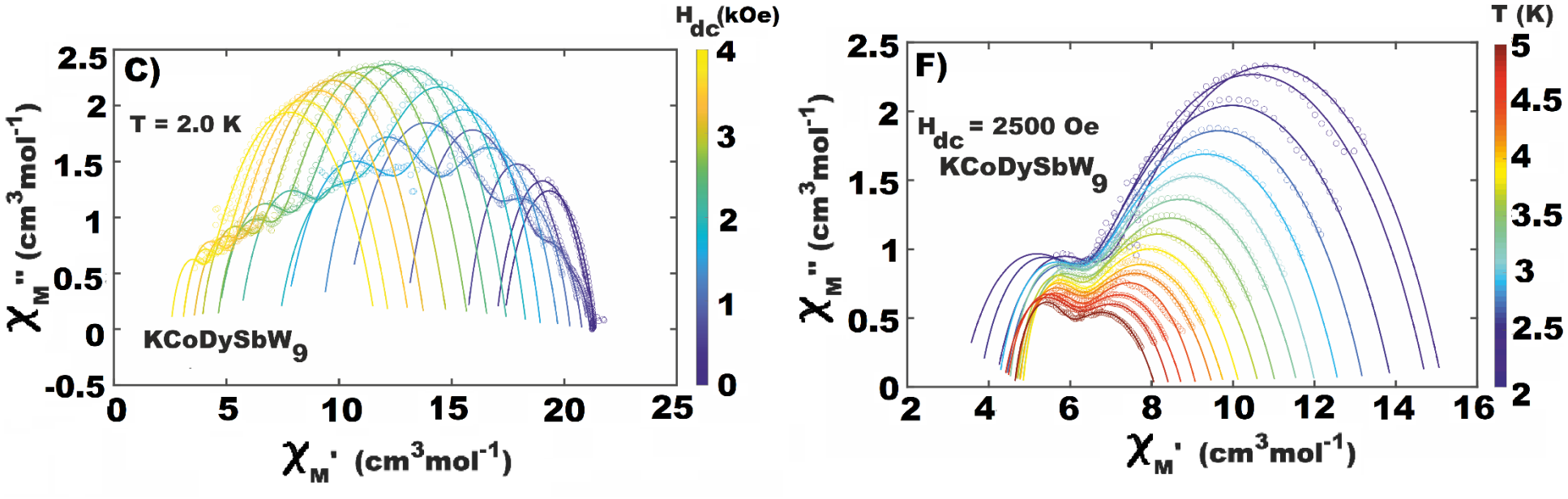

Figure S24. Field dependence (**A), B)**) and temperature dependence (**D), E)**) of ac susceptibility (H_{ac}= 3.0 Oe) and Cole-Cole plots (**C**) and **F**)) for **$KCoDySbW_9$** at indicated temperature and field. The solid lines represent the best fits according to the generalized Debye model for two relaxation processes. (**eq. S4, S5**).

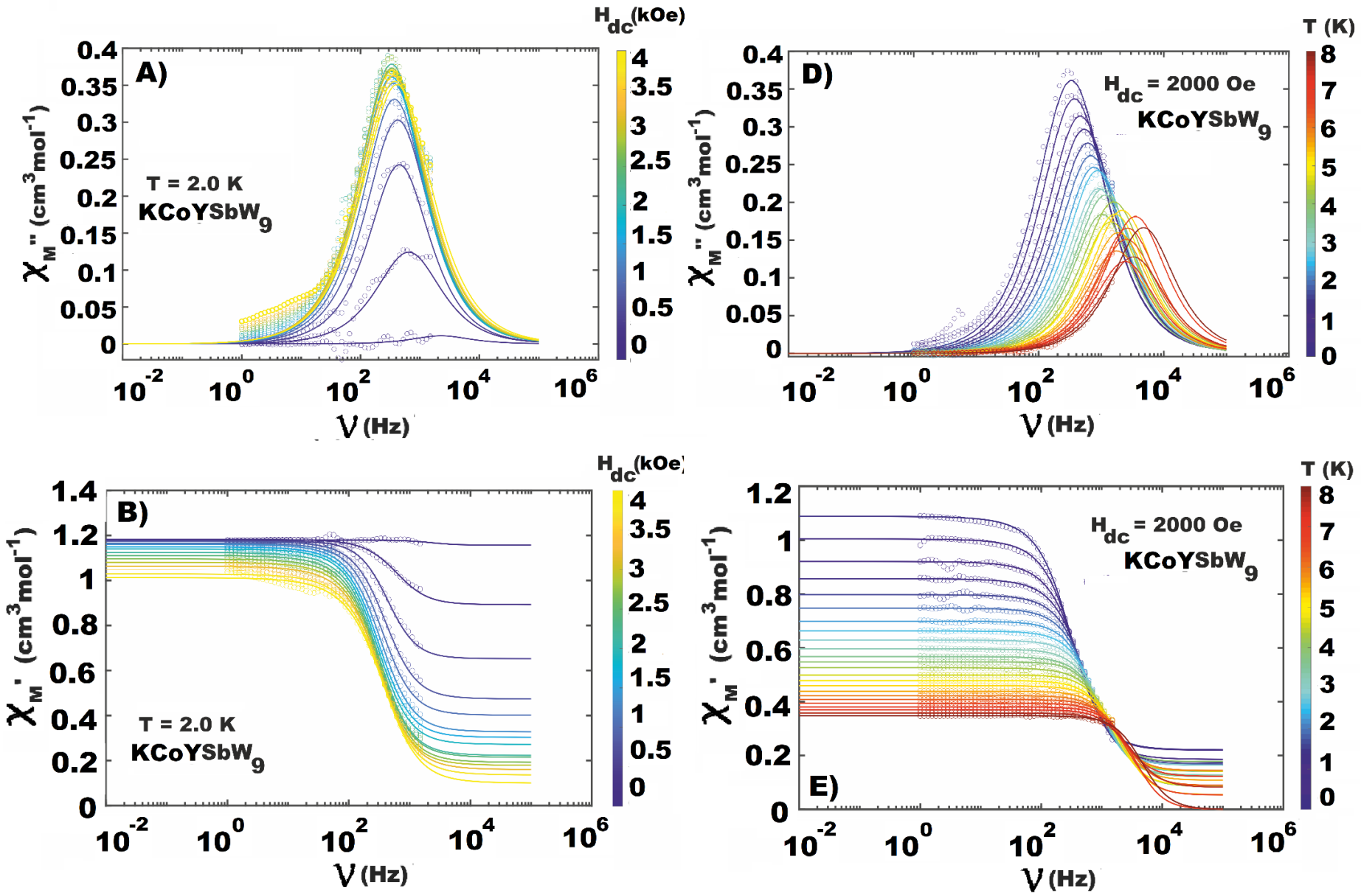
A)
T = 2.0 K
KCoYSbW9
χM'' (cm3mol-1)
ν (Hz)
Hdc(kOe)
B)
T = 2.0 K
KCoYSbW9
χM' (cm3mol-1)
ν (Hz)
Hdc(kOe)
D)
Hdc = 2000 Oe
KCoYSbW9
χM'' (cm3mol-1)
ν (Hz)
T (K)
E)
Hdc = 2000 Oe
KCoYSbW9
χM' (cm3mol-1)
ν (Hz)
T (K)

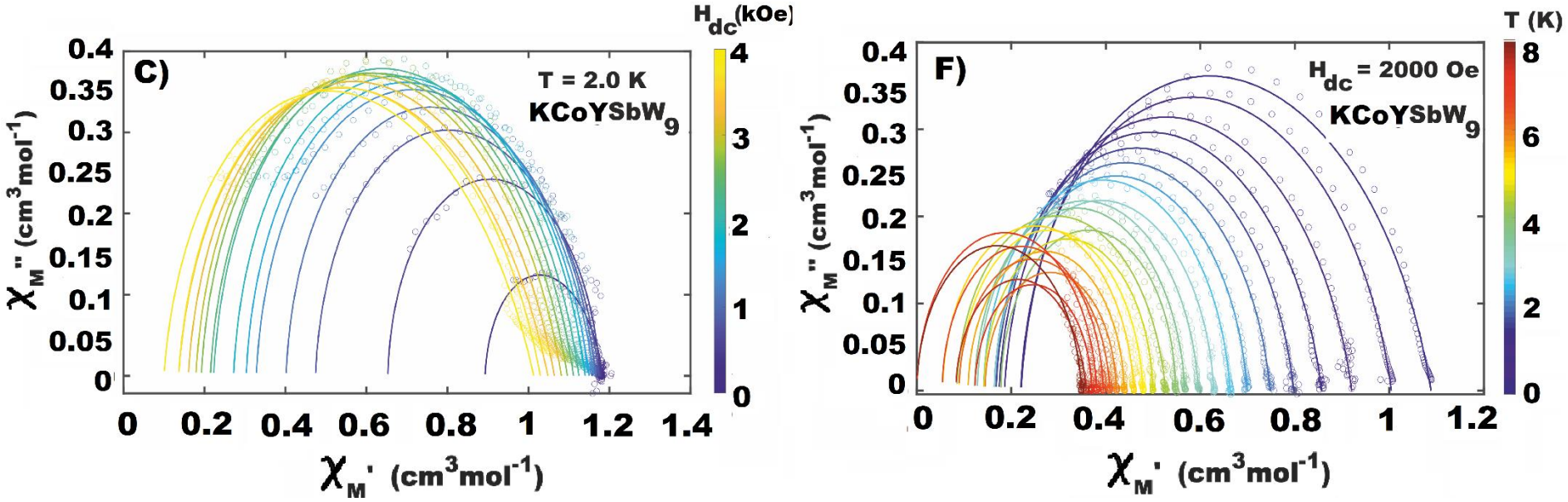

Figure S25. Field dependence (**A), B)**) and temperature dependence (**D), E)**) of ac susceptibility (H_{ac}= 3.0 Oe) and Cole-Cole plots (**C**) and **F**)) for **KCoYSbW₉** at indicated temperature and field. The solid lines represent the best fits according to the generalized Debye model for two relaxation processes. (**eq. S4, S5**).

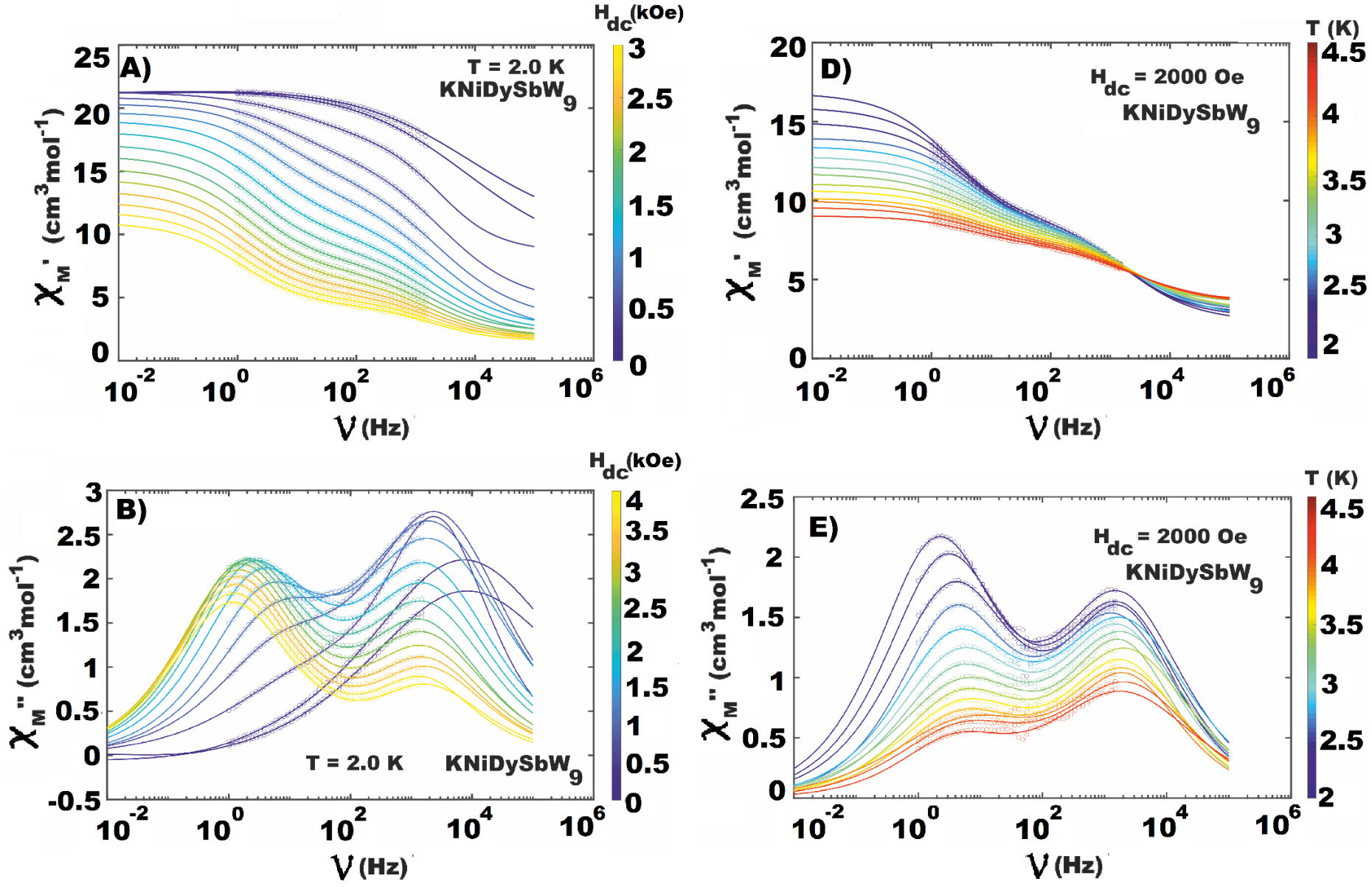
A)
T = 2.0 K
KNiDySbW9
H_dc(kOe)
χ_M' (cm³mol⁻¹)
ν (Hz)
B)
T = 2.0 K
KNiDySbW9
H_dc(kOe)
χ_M'' (cm³mol⁻¹)
ν (Hz)
D)
H_dc = 2000 Oe
KNiDySbW9
T (K)
χ_M' (cm³mol⁻¹)
ν (Hz)
E)
H_dc = 2000 Oe
KNiDySbW9
T (K)
χ_M'' (cm³mol⁻¹)
ν (Hz)

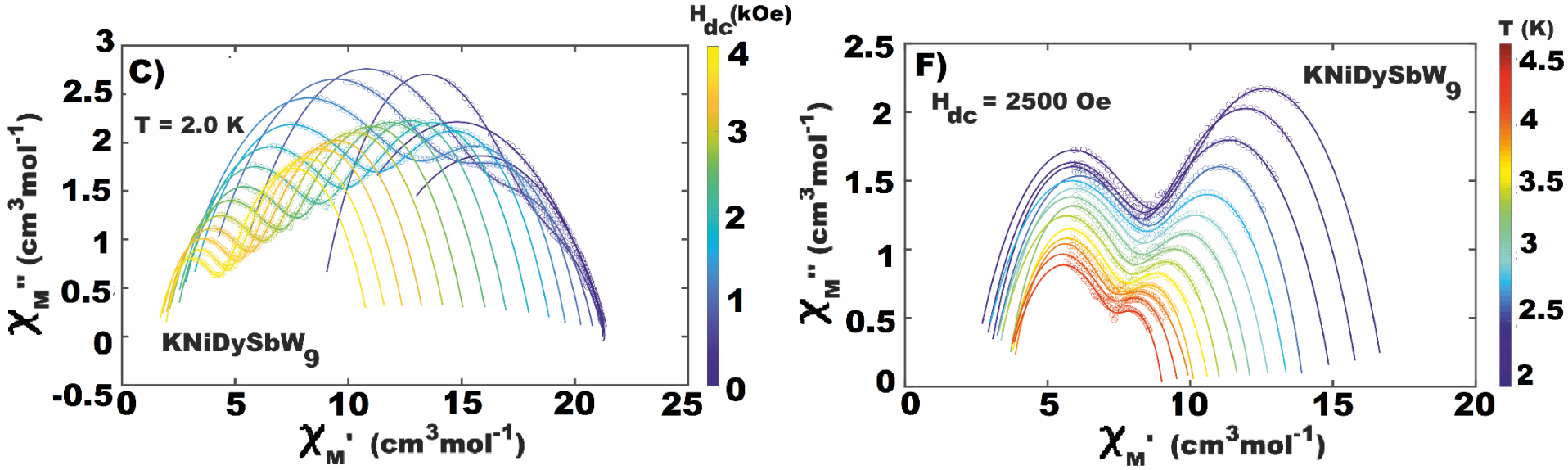

Figure S26. Field dependence (**A), B)**) and temperature dependence (**D), E)**) of ac susceptibility (H_{ac} = 3.0 Oe) and Cole-Cole plots (**C**) and **F**)) for **KNiDySbW₉** at indicated temperature and field. The solid lines represent the best fits according to the generalized Debye model for two relaxation processes. (**eq. S4, S5**).

DISPLAYED EQUATIONS

Mathematical expressions for *ac* susceptibility given by the generalized Debye model for one and two relaxation processes:

$$\chi'(\nu_{ac}) = \chi_\infty + \frac{(\chi_0 - \chi_\infty)\left[1 + (2\pi\nu_{ac}\tau)^{1-\alpha}\sin(\alpha\pi/2)\right]}{1 + 2(2\pi\nu_{ac}\tau)^{1-\alpha}\sin(\alpha\pi/2) + (2\pi\nu_{ac}\tau)^{2(1-\alpha)}} \quad \textbf{(eq-S2)}$$

$$\chi''(\nu_{ac}) = \frac{(\chi_0 - \chi_\infty)(2\pi\nu_{ac}\tau)^{1-\alpha}\cos(\alpha\pi/2)}{1 + 2(2\pi\nu_{ac}\tau)^{1-\alpha}\sin(\alpha\pi/2) + (2\pi\nu_{ac}\tau)^{2(1-\alpha)}} \quad \textbf{(eq-S3)}$$

$$\chi'(\omega) = \chi_{S,tot} + \Delta\chi_1 \frac{1+(\omega\tau_1)^{1-\alpha_1}\sin\left(\frac{\pi\alpha_1}{2}\right)}{1+(\omega\tau_1)^{1-\alpha_1}\sin\left(\frac{\pi\alpha_1}{2}\right)+(\omega\tau_1)^{(2-2\alpha_1)}} + \Delta\chi_2 \frac{1+(\omega\tau_2)^{1-\alpha_2}\sin\left(\frac{\pi\alpha_2}{2}\right)}{1+(\omega\tau_2)^{1-\alpha_2}\sin\left(\frac{\pi\alpha_2}{2}\right)+(\omega\tau_2)^{(2-2\alpha_2)}} \quad \textbf{(eq-S4)}$$

$$\chi''(\omega) = \Delta\chi_1 \frac{1+(\omega\tau_1)^{1-\alpha_1}\cos\left(\frac{\pi\alpha_1}{2}\right)}{1+(\omega\tau_1)^{1-\alpha_1}\sin\left(\frac{\pi\alpha_1}{2}\right)+(\omega\tau_1)^{(2-2\alpha_1)}} + \Delta\chi_2 \frac{1+(\omega\tau_2)^{1-\alpha_2}\cos\left(\frac{\pi\alpha_2}{2}\right)}{1+(\omega\tau_2)^{1-\alpha_2}\sin\left(\frac{\pi\alpha_2}{2}\right)+(\omega\tau_2)^{(2-2\alpha_2)}} \quad \textbf{(eq-S5)}$$

Where $\omega = 2\pi\nu$, with ν being the frequency of the applied field (s^{-1}), $\tau_{1;2}$ the corresponding relaxation time (μs), $\alpha_{1,2}$ the distribution factor and χ the corresponding susceptibility.

Table S29. The variable parameters **A**, **n**, **C**, U_{eff}, τ_0^{-1} and Q_i obtained upon application of **eq-S1** for simultaneous fit of relaxation times as function of temperature and field for **$KCoDySbW_9$** (**Fig. S27**), **$KNiDySbW_9$** (**Fig. S28**) and **$KCoYSbW_9$** (**Fig. 5**) and the corresponding R-values. Fit A represents a fit of relaxation data considering an Orbach mechanism of relaxation, whereas the relaxation data fitted in Fit B are fitted under the assumption of a Raman relaxation mechanism. The relaxation data for **$KCoYSbW_9$** was fitted assuming a direct mechanism. For all three compounds, Quantum Tunneling of Magnetization (QTM) was observed.

POM	Fit	$Q_1(s^{-1})$	$Q_2(T^{-2})$	τ^{-1} (s^{-1})	U_{eff} (K)	A ($s^{-1}K^{-1}T^{-4}$)	C ($s^{-1}K^n$)	n	R
$KCoDySbW_9$	A	2.1(2) × 10^2	1.9(4) × 10^2	1.0(2) × 10^3	9.0(6)	-	-	-	0.28
	B	2.1(3) × 10^2	1.9(5) × 10^2	-	-	-	3.2(3)	1.3(5)	0.31
$KNiDySbW_9$	A	2.1(9) × 10^3	7.7(3) ×10^2	1.5(2) × 10^2	6.5(4)	-	-	-	0.33
	B	1.2(3) × 10^3	4.2(1) × 10^3	-	-	-	1.1(3)	2.4(2)	0.47
$KCoYSbW_9$		1.8(4) × 10^3	0.6(4) × 10^2	-	-	4.0(9) ×10^3	2.4(8) × 10^2	2.3(2)	0.36

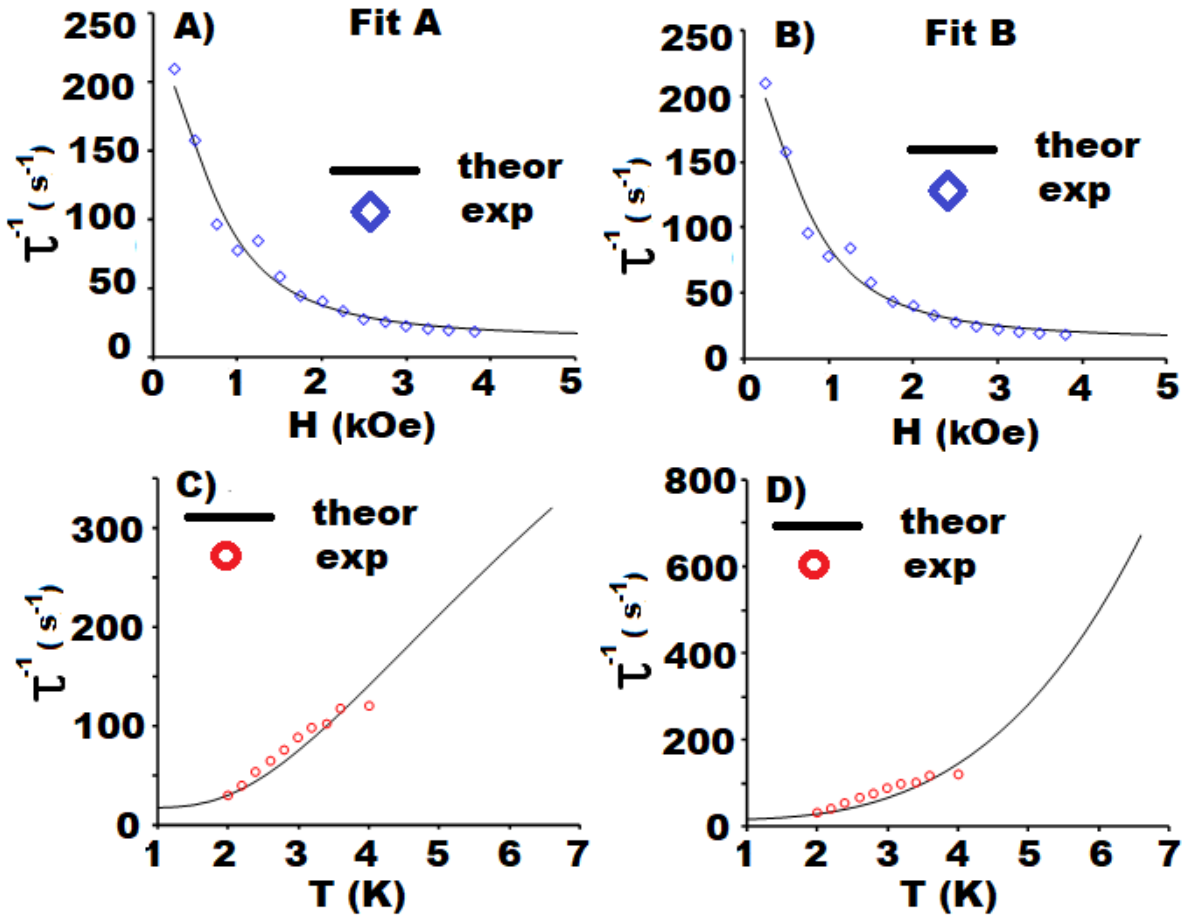

Figure S27. Field (**A), B)**) and temperature (**C), D)**) dependence of relaxation time fitted under assumption of an Orbach (**Fit A)** - and a Raman mechanism (**Fit B)** (**Table S28**) based on **eq. S1**) for **$KCoDySbW_9$.**

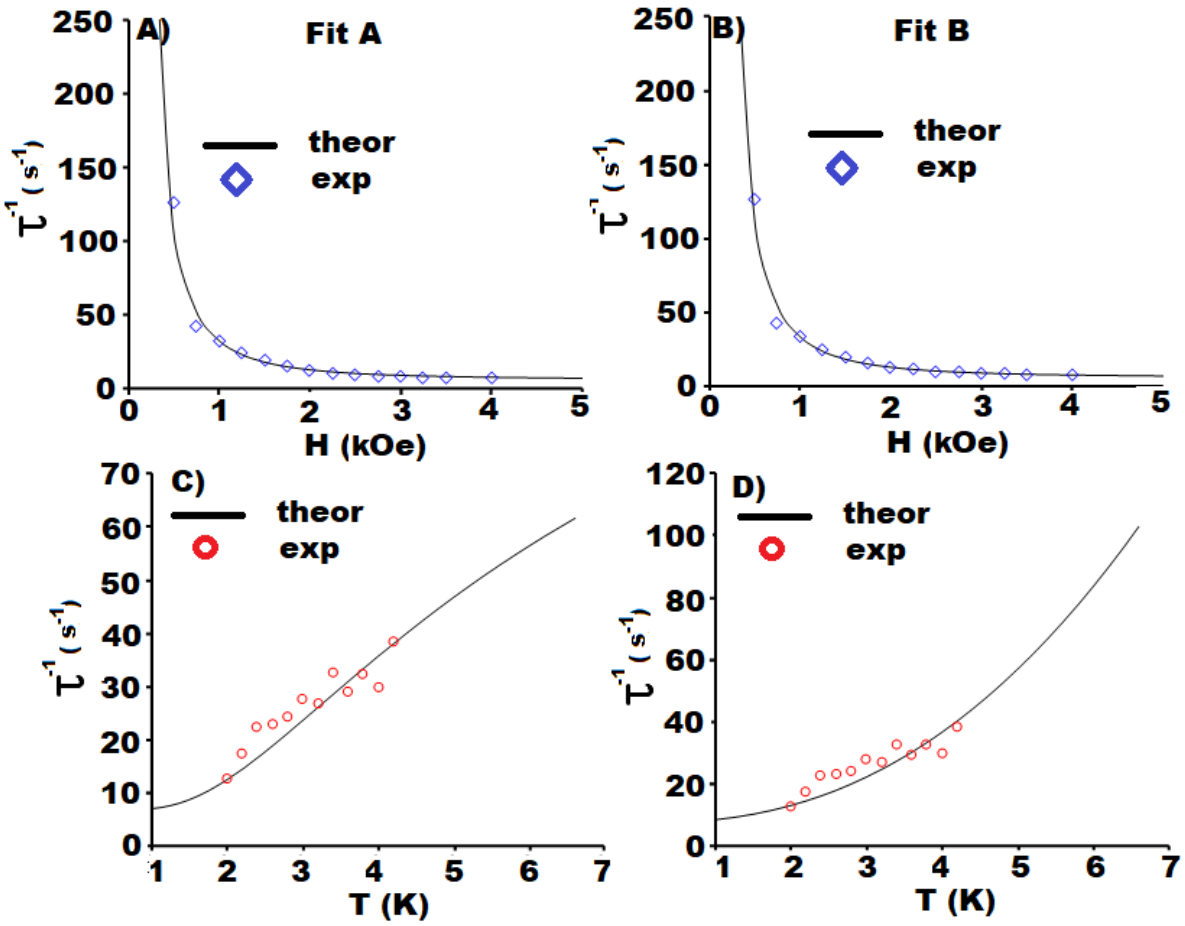

Figure S28. Field (**A), B)**) and temperature (**C), D)**) dependence of relaxation time fitted under assumption of an Orbach (**Fit A)** - and a Raman mechanism (**Fit B)** (**Table S28**) based on **eq. S1**) for **$KNiDySbW_9$.**

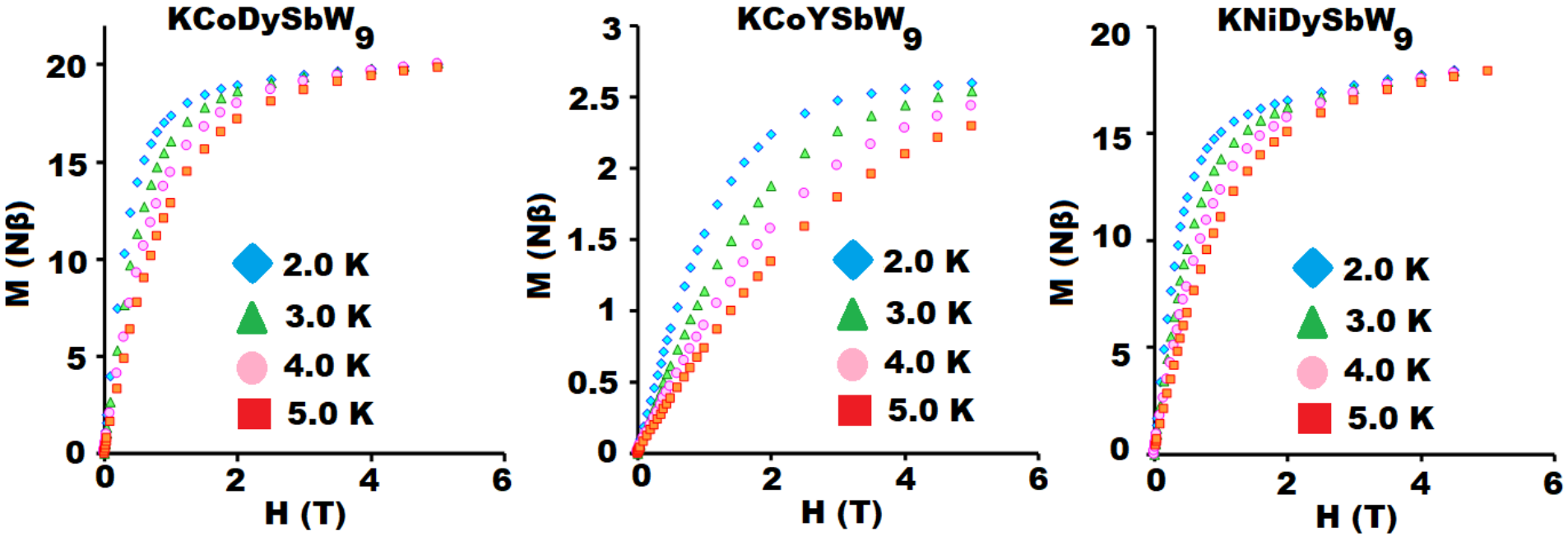

Figure S29. Magnetization curves measured between 0 and 5 T at different temperatures for **KCoDySbW$_9$**, **KNiDySbW$_9$** and **KCoYSbW$_9$**.

References

1 M. Bösing, I. Loose, H. Pohlmann, B. Krebs. New Strategies for the Generation of Large Heteropolymetalate Clusters: The β-*B*-SbW_9 Fragment as a Multifunctional Unit. *Chem.– Eur. J.*, **1997**, *3*, 1232−1237.

2 M. Ibrahim, S. Sankar Mal, B. S. Bassil, A. Banerjee, U. Kortz. Yttrium (III)-Containing Tungstoantimonate(III) Stabilized by Tetrahedral WO_4^{2-} Capping Unit, $[\{Y(\alpha\text{-}SbW_9O_{31}(OH)_2)(CH_3COO)(H_2O)\}_3(WO_4)]^{17-}$ *Inorg. Chem.* **2011**, *50*, 956–960.

3 Bruker SAINT v7.68A Copyright © 2005-2016 Bruker AXS.

4 G.M. Sheldrick SADABS University of Göttingen, Germany (1996).

5 G. M Sheldrick. (1996). SHELXS. University of Göttingen, Germany.

6 G. M Sheldrick. (1996). SHELXL. University of Göttingen, Germany.

7 O. V. Dolomanov, L. J. Bourhis, R. J., Gildea, J. A. K. Howard, H. Puschmann, OLEX2, *J. Appl. Cryst.,* **2009**, *42*, 339-341.

8 C. B. Huebschle, G. M. Sheldrick, B. Dittrich, ShelXle: a Qt graphical user interface for SHELXL, *J. Appl. Cryst*., **2011,** *44*, 1281-1284.

9 P. Pascal. Recherches Magnetochimiques. *Ann. Chim. Phys.* **1910**, *19*, 5–70.

10 O. Kahn. *Molecular Magnetism*; **1993**.

11 D. Gatteschi, R. Sessoli Villain in Molecular Nanomagnets, Vol. 1. *Oxford Univ. Press, Oxford*, **2006**; 376.

12 Y. Chen, L. Sun, S. Chang, L. Chen, J. Zhao. Synergistic Effect between Different Coordination Geometries of Lanthanides and Various Coordination Modes of 2-Picolinic Acid Ligands Tuning Three Types of Rare 3d–4f Heterometallic Tungstoantimonates. *Inorg. Chem.* **2018**, *57*, 15079−15092.

13 J. Cai, X.-Y. Zheng, J. Xie, Z.-H. Yan, X.-J. Kong, Y.-P. Ren, L.-S. Long, L.-S. Zheng. Anion-Dependent Assembly of Heterometallic 3d–4f Clusters Based on a Lacunary Polyoxometalate. *Inorg. Chem*. **2017**, *56*, 8439−8445.

14 B. Artetxe, S. Reinoso, L. S. Felices, L. Lezama, J. M. Gutierrez-Zorilla, C. Vincent, F. Haso, T. Liu. New Perspectives for Old Clusters: Anderson–Evans Anions as Building Blocks of Large Polyoxometalate Frameworks in a Series of Heterometallic 3 d–4 f Species. *Chem.- Eur. J.* **2016**, *22*, 4616–4625.

15 X. Ma, K. Song, J. Cao, P. Gong, H. Li, L. Chen, J. Zhao. Synthesis, structure and electrochemical properties of a Fe^{III}–Ce^{III} heterometallic sandwich-type tungstoantimonate with novel 2-D infinite structure $[Ce(H_2O)_8][Ce(H_2O)_6][Fe_4(H_2O)_{10}(B\text{-}\beta\text{-}SbW_9O_{33})_2]\cdot 16\ H_2O$. *Inorg. Chem. Commun*. **2015**, *60*, 65-70.

16 X. Feng, J. L. Liu, K. S. Pedersen, J. Nehrkorn, A. Schnegg, K. Holldack, J. Bendix, M. Sigrist, H. Mutka, D. Samohvalov. Multifaceted Magnetization Dynamics in the Mononuclear Complex $[Re^{IV}Cl_4(CN)_2]^{2-}$. *Chem. Commun*. **2016**, *52*, 12905–12908.